An investigation of the reduction in aqueous acetonitrile of 4-methoxybenzenediazonium ion by the tetrakis(acetonitrile)Cu(I) cation catalysed by hydrogenphosphate dianion†‡

Peter Hanson,* Alec B. Taylor, Paul H. Walton and Allan W. Timms§

Received 18th October 2006, Accepted 8th December 2006
First published as an Advance Article on the web 15th January 2007
DOI: 10.1039/b615211b

In aqueous acetonitrile containing a phosphate buffer, 4-methoxybenzenediazonium ion is reduced by one or more of the partially aquated cations derived from tetrakis(acetonitrile)Cu(I) cation in this medium. Investigation of the reaction mechanism indicates the rate determining step to be the association of the diazonium ion with the hydrogenphosphate dianion to give an adduct which then undergoes reduction by Cu(I). The reaction gives a range of products which have been identified and quantified by GC. One of these, 4-methoxyphenol was unexpected in the reducing conditions; its presence could be explained by the disproportionation of a 4-methoxyphenylcopper(II) complex giving bis(4-methoxyphenyl)copper(III) which reacts with water to produce the phenol and an equivalent amount of methoxybenzene. A scheme is proposed which accounts for all the observed products and computer modelling gives a satisfactory description of the distributions of the five major products as functions of the relative proportions of the reactants for dilute conditions and those where the reductant is in excess. When the diazonium ion is in excess, the behaviour of the model and the experimental reactant accountability suggest the occurrence of additional reactions which give products unobserved by GC.

Introduction

It has long been known that Sandmeyer reactions may be accompanied by the formation of characteristic by-products, namely, azoarenes, biaryls and the reduction products of the initial diazonium ions.[2] The substitution patterns of these substances show that their respective Ar–N, Ar–Ar and Ar–H bonds replace the bond to the original diazonium group. It is believed that the by-products arise by leakage of aryl radicals from the Sandmeyer catalytic cycle[3] (Scheme 1) and that their formation involves, at least in part, the mediation of organocopper intermediates.[3b,4]

Thirty years ago, Cohen and co-workers[5] investigated the reaction of 4-nitrobenzenediazonium tetrafluoroborate with tetrakis(acetonitrile)copper(I) perchlorate in acetone. Lacking transferable ligands on the copper, this reaction gives the characteristic Sandmeyer by-products as its main products and Cohen and co-workers found evidence for the involvement of organocopper intermediates in the response of the product distribution to variation in conditions. A mechanism based on their observations and on contemporaneous work demonstrating the capture of alkyl radicals by copper ions to form transient organocopper intermediates,[6] was proposed for the formation of products. The investigation was confined to the product-forming steps, no attention being given to the initial rate-determining reduction.

Department of Chemistry, University of York, Heslington, York, UK YO10 5DD

† Sandmeyer reactions. Part 9. For part 8 see ref. 1.

‡ Electronic supplementary information (ESI) available: Preparation and characterisation of reaction media; kinetic measurements (figures); nitrogen evolution measurements; simulated product distributions; adaptation of the model for change of substituent character. See DOI: 10.1039/b615211b

§ Formerly at Great Lakes Fine Chemicals Limited, when at Halebank, Widnes, UK WA8 8NS.

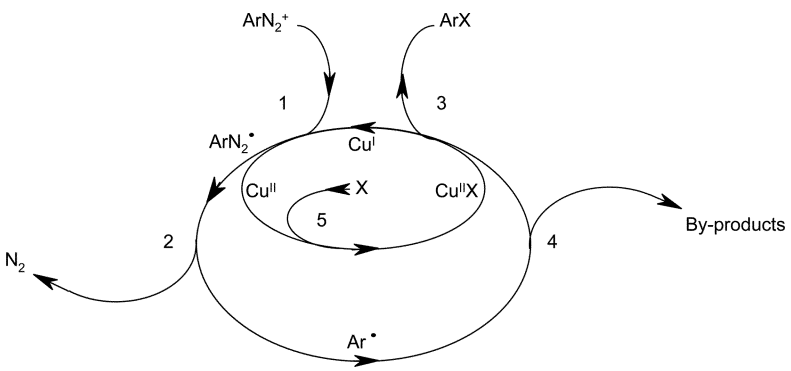

Scheme 1

We have provided evidence[7] that the reduction steps of Sandmeyer reactions are inner-sphere processes requiring bond formation between the β-nitrogen of the diazonium ion and a ligand on the Cu(I) reductant. For the formation of such a bond, a lone-pair is required on the ligand. The acetonitrile ligands on Cohen's reductant have no such lone-pair and we were interested to know how reduction of diazonium ions occurs. Furthermore, in the time intervening since the work of Cohen and his group, more kinetic information has become available[8–12] regarding radical/copper ion reactions and the possibility arises of testing the adequacy of proposed reaction schemes by computer simulation. The purpose of this paper is therefore twofold: to report an investigation into the mechanism of reaction between 4-methoxybenzenediazonium ion, **1**, and tetrakis(acetonitrile)copper(I), **2**, both cations as their tetrafluoroborate salts and to interpret experimental product distributions from this reaction in the light of simulation studies.

Results

(i) Choice of diazonium ion

The diazonium ion, **1**, was chosen on account of several advantages conferred by its electron-donating substituent. Such substitution suppresses the formation of diazoates in the neutral and mildly basic aqueous media of our experiments[13] and ensures the diazonium ion does not undergo significant heterolysis at 298 K.[14] Both of these processes would have potential for complicating investigation of the homolytic reduction of interest. Additionally, the choice of a weakly electrophilic diazonium ion ensures that its reduction is comparatively slow which facilitates simple spectrophotometric monitoring. It is known that the relative yield of the binuclear products varies with the type of substitution, azoarene being favoured over biaryl by electron-donation and *vice versa* by electron-withdrawal.[2] The choice of a substrate with an electron-donating substituent therefore allows our study to complement rather than supplement the previous one.

(ii) The reductant

The salt $[Cu^{I}(NCMe)_4]BF_4$, **2**, is readily prepared[15] and, being stable in solutions containing MeCN, can be used conveniently in kinetic studies where the use of Cu^{+}_{aq} would be difficult due to its ready autoxidation and disproportionation. The standard reduction potential [Cu(II)/Cu(I)]of **2** in MeCN has been given as 0.98 V *vs.* SCE[16] (*i.e.* 1.224 V *vs.* NHE)[17] exceeding the threshold of ~1 V above which reductants fail to reduce diazonium ions.[18] Consistently, spectrophotometrically we observed no perceptible reaction at 298 K when **1** (7.5×10^{-5} mol dm^{-3}) was treated with a 20-fold excess of **2** in MeCN. For their study using acetone as solvent, Cohen and co-workers[5] had found it necessary to include a low percentage of water in order to observe reduction of 4-nitrobenzenediazonium ion which is more electrophilic than **1**. Although crystallising from MeCN with four MeCN ligands,[19] in aqueous MeCN the copper(I) cation exists in forms having fewer such ligands, $[Cu^{I}(NCMe)_n(OH_2)_{(4-n)}]^{+}$, ($n$, 1–3).[20] These complexes are expected to exhibit reduction potentials falling between that of **2** (1.224 V *vs.* NHE) and that of the Cu^{2+}_{aq}/Cu^{+}_{aq} couple (0.159 V *vs.* NHE)[21] and hence to be better reductants than **2** itself.[22] Also, the water ligands possess lone pairs which might bridge to diazonium ions; nevertheless, spectrophotometrically we found no perceptible reaction at 298 K when **1** (7.5×10^{-5} mol dm^{-3}) was treated with a 20-fold excess of **2** in 50% v/v aqueous MeCN. There was, however, a slow, incomplete evolution of nitrogen (14% of the theoretical yield in 15 min) when **1** and **2**, both 0.01 mol dm^{-3}, were reacted at 298 K in the same solvent.

(iii) The reaction medium

In the above gasometric experiment, the pH of the solvent mixture fell from 7.3 to 4.0 over the duration of the experiment. Previously,[23] we had found that the kinetic behaviour of the Sandmeyer cyanation of **1** became amenable to measurement when carried out in a 50% v/v mixture of acetonitrile with a pH 7 aqueous buffer. The reaction of **1** with **2** in this medium was therefore investigated. At both spectrophotometric and gasometric concentrations the reaction was found to proceed smoothly. At the latter, higher, concentration, the solution acquired a deep orange colour due to the formation of 4,4′-dimethoxyazobenzene and a pale blue precipitate also formed which we treat as $CuHPO_4$ (see below). At spectrophotometric concentrations of the reactants, no perceptible colouration developed and there was no precipitation during the course of the reaction. (In some instances an onset of turbidity was noticeable at the end of reaction and, on prolonged standing, precipitation occurred.) The dilution of aqueous buffer solutions with MeCN results in a significant endotherm and an associated contraction in the volume of solution. For kinetic measurements it is therefore necessary to premix and thermally equilibrate solvents before initiation of reaction by means which produce negligible additional perturbation.

The pH values measured for mixtures of aqueous buffers with acetonitrile are higher than those measured for the buffers alone. For the determination of pH and buffer ratios in aqueous MeCN media, we have relied on data published by Barbosa and co-workers.[24] The key parameters we have used and which are interpolated from their results are given in Table 1. [Details of buffer preparation and characterisation are given in ESI.‡] In the interest of clarity we distinguish pH values, concentrations of buffer components and other properties in aqueous MeCN from those in purely aqueous buffers by subscripting the volume percentage 'V' of MeCN, or 'aq' as appropriate.

(iv) Dependence of reaction rate on buffer concentration

In either MeCN alone or in mixtures of MeCN with phosphate buffers (pH_{aq} 6–7.5), **1** absorbs at λ_{max} 312 nm; log (ε/dm^2 mol^{-1}) = 3.39 in aqueous MeCN, B_{50} = [total phosphate]$_{50}$ = 0.025 mol dm^{-3}, pH_{50} = 7.99. In the presence of an excess of **2**, which does not absorb significantly at this wavelength, the absorbance decays in a pseudo-first order manner and is readily monitored spectrophotometrically (ESI, Fig. S1‡).

Pseudo-first order rate constants k_{obs} (see Table 2) were measured for several different initial concentrations of **2** and different concentrations of phosphate buffer in 50% v/v aqueous MeCN. The linearity of plots of k_{obs} as a function of the initial concentration of **2** shows the reaction to be of first order in Cu(I) and the separate plots for the different concentrations of buffer of the same pH_{aq} implicate one or more buffer components in the reaction also (ESI, Fig. S2). At a given pH, the total buffer

Table 1 Interpolated properties at 298 K of aqueous acetonitrile mixtures and derived solutions[a]

Property	Percentage v/v MeCN *V*: 0	20	30	50	Ref.
Density, ρ_V/g cm^{-3}	0.9971	0.9688	0.9511	0.9060	24*a*
Debye–Hückel coefficient, A_V/(mol kg^{-1})$^{1/2}$	0.5103	0.5699	0.6167	0.7523	24*a*,*b*
Relative permittivity, ε_{rV}	78.36	71.80	67.83	58.76	24*a*,*b*
Viscosity, $10^4\eta$/kg m^{-1} s^{-1}	8.903	9.754	9.615	8.347	25
Autoprotolysis, pK_{apV}	14.00	14.45	14.74	15.48	24*a*,*b*
$H_2PO_4^-$, pK_{aV}	7.20	7.65	7.87	8.35	24*c*
Standard buffers					24*d*,*e*
pH_{SV}(phthalate)[b]	4.00	4.54	4.85	5.45	
pH_{SV}(phosphate)[c]	6.86	7.36	7.55	7.73	
pH_{SV}(borate)[d]	9.18	9.87	10.23	10.96	

[a] See ESI for details of interpolation. [b] Potassium hydrogenphthalate, 0.05 mol kg^{-1}. [c] KH_2PO_4 and Na_2HPO_4, each 0.025 mol kg^{-1}. [d] $Na_2B_4O_7{\cdot}10H_2O$, 0.01 mol kg^{-1}.

Table 2 Observed pseudo-first order rate constants (10^3k_{obs}/s^{-1})[a] for the reduction of 4-methoxybenzenediazonium ion[b] by tetrakis(acetonitrile)copper(I) in 50% aqueous acetonitrile phosphate buffers

	Buffer						
	B_{50}[d]:	0.005[e]	0.0125[e]	0.025[e]	0.0375[e]	0.05[e]	0.05[f]
10^4[**2**]$_{init}$/mol dm^{-3}[c]	pH_{50}[g]:	8.15	8.10	7.99	7.95	7.92	6.92
3.726				2.22 ± 0.24	4.02 ± 0.10	5.20 ± 0.31	
5.982						11.61 ± 1.05	
7.505			3.14 ± 0.25	6.61 ± 0.42	10.69 ± 0.46	14.34 ± 0.82	
8.960						17.49 ± 0.89	
10.41						20.67 ± 0.97	
11.20			4.69 ± 0.50	10.45 ± 1.80	17.27 ± 0.66	21.14 ± 0.13	
14.89			6.22 ± 0.40	13.68 ± 1.74	23.72 ± 1.80	30.93 ± 0.54	1.98 ± 0.06
18.56		0.45 ± 0.07	7.35 ± 0.73	17.78 ± 1.20	30.35 ± 1.13	38.86 ± 2.50	2.66 ± 0.09
22.22		0.60 ± 0.01	8.82 ± 0.40		35.16 ± 1.27		3.08 ± 0.07
25.93		0.77 ± 0.01					3.57 ± 0.03
29.56							4.01 ± 0.05

[a] Uncertainties are the standard deviations of the sets of measurements of each rate constant. [b] Cuvette concentration = 7.5×10^{-5} mol dm^{-3}. [c] Cuvette concentrations. [d] Molar concentration of buffer salt in 50% aqueous acetonitrile. [e] Nominal pH_{aq} 7. [f] Nominal pH_{aq} 6. [g] Measured pH for 50% aqueous acetonitrile buffer.

concentration, B_{50}, can be expressed as a function of either relevant anion *via* the buffer ratio, r_{B50}:

$$B_{50} = \{[H_2PO_4^-]_{50} + [HPO_4^{2-}]_{50}\} = (1 + r_{B50})[HPO_4^{2-}]_{50} \equiv (1 + r_{B50}^{-1})[H_2PO_4^-]_{50}$$

a particular ion is hence not directly identifiable. However, the fact that the values of k_{obs} are smaller when determined in buffer $B_{50} = 0.05$ mol dm^{-3}, $pH_{50} = 6.92$ than those determined in buffer $B_{50} = 0.05$ mol dm^{-3}, $pH_{50} = 7.92$, suggests HPO_4^{2-} may have the dominant role (*cf.* Table 2, columns 6 and 7). Plots of k_{obs} *versus* $[HPO_4^{2-}]_{50}$ are linear (ESI, Fig. S3), the linearity indicating a first order dependence on this species also; this choice of buffer component will be justified more fully later [section (vi)]. Table 3 collects the second order rate constants $k_{2(Cu)}$ and $k_{2(P2)}$ measured as the gradients of the plots of k_{obs} *versus* the initial concentrations of **2** and the hydrogenphosphate dianion, respectively.

Table 3 Collected second order rate constants for the reduction of 4-methoxybenzenediazonium ion by tetrakis(acetonitrile)copper(I) in 50% v/v aqueous MeCN buffers with derived third order constants[a]

Entry	B_{50}/mol dm^{-3}[b]	$[HPO_4^{2-}]$/mol dm^{-3}[c]	$k_{2(Cu)}$/dm^3 mol^{-1} s^{-1}[d]	Entry	10^4[**2**]$_{init}$/mol dm^{-3}	$k_{2(P2)}$/dm^3 mol^{-1} s^{-1}[e]
1	0.005	0.00193	0.44 ± 0.04[f]	7	3.726	0.48 ± 0.05[f]
2	0.0125	0.00450	3.81 ± 0.35	8	7.505	1.22 ± 0.11
3	0.025	0.00760	10.31 ± 0.84	9	11.20	1.82 ± 0.58
4	0.0375	0.01068	17.10 ± 1.02	10	14.89	2.51 ± 0.48
5	0.05	0.01354	22.29 ± 1.29	11	18.56	3.20 ± 0.43
6	0.05	0.00179	1.35 ± 0.22	12	22.22	3.79 ± 0.38[f]
	$k_{3(P2)} = (1835 \pm 250)$ dm^6 mol^{-2} s^{-1}				$k_{3(Cu)} = (1792 \pm 65)$ dm^6 mol^{-2} s^{-1}	

[a] The uncertainties are the 95% confidence intervals except where otherwise indicated. [b] Total concentration of buffer salt in 50% v/v aqueous MeCN. [c] Concentrations calculated as $B_{50}/(1 + r_{B50})$ where r_{B50} is the buffer ratio calculated from pK_{a50} (see Table 1) and the measured pH_{50} (see header to Table 2). [d] Gradients of k_{obs} *versus* [**2**]$_{init}$ plots (Fig. 2). [e] Gradients of k_{obs} *versus* $[HPO_4^{2-}]$ plots (Fig. 3). [f] Uncertainty given as 10% of value.

Self-consistent third order rate constants are found when $k_{2(Cu)}$ is plotted as a function of $[HPO_4^{2-}]_{50}$ or $k_{2(P2)}$ is plotted as a function of $[\mathbf{2}]_{init}$: the former gives $k_{3(P2)} = (1835 \pm 248)$ dm^6 mol^{-2} s^{-1} whereas the latter gives $k_{3(Cu)} = (1792 \pm 65)$ dm^6 mol^{-2} s^{-1} whence a mean third order constant for reaction in 50% aqueous MeCN of $k_{3(50)} = (1.81 \pm 0.13) \times 10^3$ dm^6 mol^{-2} s^{-1}.

(v) Dependence of reaction rate on ionic strength

A series of aqueous buffer solutions of nominal pH_{aq} 7 (B_{aq} = 0.075 mol dm^{-3}) was prepared in which the ionic strength was increased from the intrinsic value by addition of KNO_3. On dilution with MeCN (50% v/v), the ionic strengths were corrected for the volume change, for the associated decrease in solvent density (see Table 1) and for the effect of the medium change on the buffer ratio indicated by the increase in measured pH. The mean pH_{50} value of 7.85 was used to obtain a single buffer ratio $r_{B50} = 3.162$ [*i.e.* antilog ($pK_{a50} - pH_{50}$) = antilog (8.35 − 7.85)] for the latter correction to ionic strength. Pseudo-first order rate constants for reductions at 298 K of **1** (7.5×10^{-5} mol dm^{-3}) by **2** (1.489×10^{-3} mol dm^{-3}), measured in the buffer solutions so prepared, are given in Table 4.

Assuming the Debye–Hückel limiting law for the definition of activity coefficients, the rate constant, k, of a simple reaction between ionic reactants is related to ionic strength, I, by eqn (1) where k° is the rate constant when the activity coefficients are 1, z_i and z_j are the charges of the reacting ions and the Debye–Hückel coefficient A is characteristic of the solvent[26] (A_V values for aqueous MeCN media are given in Table 1).

$$\log k = \log k^\circ + 2Az_iz_j\sqrt{I} \quad (1)$$

Log k_{obs} was found to vary linearly with $(I_{50}/\text{mol kg}^{-1})^{1/2}$, the gradient of the graph, *i.e.* $2A_{50}z_iz_j$, being $-(3.086 \pm 0.244)$ where the uncertainty is the 95% confidence interval (ESI, Fig. S4‡). Taking $A_{50}/(\text{mol kg}^{-1})^{1/2} = 0.7523$ (Table 1), it follows from the negative gradient that $z_iz_j = -(2.05 \pm 0.16)$ and hence that z_i and z_j must have *opposite* signs.[27] The rate determining step of the reaction therefore cannot involve reaction of **1** with other cations such as $[Cu^I(NCMe)_n(OH_2)_{(4-n)}]^+$, ($n$, 1–3) or with neutral species such as $[Cu^IOH(NCMe)_n(OH_2)_{(3-n)}]$, ($n$, 1–3); it must involve a doubly charged ion and a singly, oppositely charged ion, evidently HPO_4^{2-} and either **1** or one or more of $[Cu^I(NCMe)_n(OH_2)_{(4-n)}]$, ($n$, 1–3).

(vi) Apparent dependence of reaction rate upon pH at constant ionic strength

Rate constants for the reduction of **1** (7.5×10^{-5} mol dm^{-3}) by **2** (1.489×10^{-3} mol dm^{-3}) were measured in a series of experiments where the buffer pH was varied at constant ionic strength [see Experimental (iv)]. As with the buffers at intrinsic ionic strength, when diluted with MeCN the pH values measured for these buffers (pH_{50}) were increased. The results are given in Table 5.

Table 4 Variation with ionic strength of pseudo-first order rate constants (k_{obs}) for the reduction of 4-methoxybenzenediazonium ion by tetrakis(acetonitrile)copper(I) in 50% aqueous acetonitrile phosphate buffers

$[KNO_3]$/mol dm^{-3} [a]	I_{aq}/mol dm^{-3} [b]	pH_{50} [c]	I_{50}/mol kg^{-1} [d]	10^2k_{obs}/s^{-1} [e]
0.00	0.162[f]	7.95	0.061	2.37 ± 0.18
0.02	0.182	7.90	0.072	1.94 ± 0.05
0.04	0.202	7.87	0.083	1.72 ± 0.10
0.06	0.222	7.83	0.094	1.56 ± 0.06
0.08	0.242	7.82	0.105	1.32 ± 0.03
0.10	0.262	7.79	0.116	1.19 ± 0.04
0.12	0.282	7.76	0.127	1.08 ± 0.01

[a] Concentration added to aqueous buffer, B_{aq} = 0.075 mol dm^{-3}, pH 7.00. [b] Ionic strength of pH 7 aqueous buffer. [c] pH measured for buffer in 50% aqueous MeCN (B_{50} = 0.0375 mol dm^{-3}) shows a small variation with ionic strength; the mean value 7.85 was used to calculate a single buffer ratio $r_{B50} = 3.162$. [d] Ionic strength of buffer in 50% v/v aqueous MeCN corrected for dilution, change in buffer ratio and solvent density change. [e] Each value is the average of at least three determinations in which **1** (7.5×10^{-5} mol dm^{-3}) was reduced by **2** (1.489×10^{-3} mol dm^{-3}) at 298 K; the uncertainty is the standard deviation of the set of measurements of each rate constant. [f] Intrinsic value.

Table 5 Variation with pH at constant ionic strength[a] of the pseudo-first order rate constants (k_{obs}) for the reduction of 4-methoxybenzenediazonium ion by tetrakis(acetonitrile)copper(I) in 50% aqueous acetonitrile phosphate buffer

pH_{aq} [b]	10^2B_{50}/mol dm^{-3} [c]	pH_{50} [d]	r_{B50} [e]	$10^2[H_2PO_4^-]_{50}$/mol dm^{-3} [f]	$10^3[HPO_4^{2-}]_{50}$/mol dm^{-3} [f]	$10^9[OH^-]_{50}$/mol dm^{-3} [g]	10^3k_{obs}/s^{-1} [h]
6.00(6.07)	6.623	6.95	25.119	6.369	2.536	2.95	3.67 ± 0.10
6.25(6.31)	4.167	7.09	18.197	3.949	2.170	4.07	4.03 ± 0.09
6.50(6.54)	2.778	7.35	10.000	2.525	2.525	7.41	4.33 ± 0.11
6.75(6.76)	2.000	7.63	5.248	1.680	3.201	14.12	5.06 ± 0.12
7.00(7.01)	1.562	7.92	2.692	1.139	4.233	27.54	5.59 ± 0.18
7.25(7.28)	1.316	8.18	1.479	0.785	5.308	50.12	6.97 ± 0.05
7.50(7.53)	1.178	8.43	0.832	0.535	6.430	89.13	8.23 ± 0.50

[a] The ionic strength, I_{aq}, of each of the initial aqueous buffers was adjusted to 0.2 mol dm^{-3} with KNO_3; twofold dilution with MeCN modifies the buffer ratio with the result that I_{50} lies in the narrow range 0.089 ± 0.005 mol dm^{-3}. [b] Nominal value (measured value). [c] Total buffer salt concentration ($[KH_2PO_4] + [K_2HPO_4]$) in 50% aqueous MeCN [see Experimental (iv)]. [d] Values measured for 50% aqueous MeCN buffers. [e] Buffer ratios of 50% aqueous MeCN buffers calculated as r_{B50} = antilog ($pK_{a50} - pH_{50}$) (see Table 1). [f] Ionic concentrations in 50% aqueous MeCN buffers calculated from B_{50} and r_{B50}. [g] Ionic concentrations in 50% aqueous MeCN buffers calculated as $[OH^-]_{50}$ = antilog ($pH_{50} - pK_{ap50}$) (see Table 1). [h] Each value is the average of at least three determinations in which **1** (7.5×10^{-5} mol dm^{-3}) was reduced by **2** (1.489×10^{-3} mol dm^{-3}); the uncertainty is the standard deviation of the set of measurements of each rate constant.

For each aqueous buffer, the total concentration, B_{aq}, of the buffering ions ($[H_2PO_4^-]_{aq} + [HPO_4^{2-}]_{aq}$) was known. The individual concentrations of these ions in the 50% aqueous MeCN buffer were obtained as $B_{50}/(1 + r_{B50}^{-1})$ and $B_{50}/(1 + r_{B50})$, respectively, where $B_{50} = 0.5B_{aq}$ and r_{B50} is the buffer ratio calculated as antilog ($pK_{a50} - pH_{50}$), pK_{a50} being 8.35 (see Table 1). Table 5 also includes values of $[OH^-]_{50}$ calculated as antilog ($pK_{ap50} - pH_{50}$) with $pK_{ap50} = 15.48$ (see Table 1). The dependence of k_{obs} upon the concentrations of basic species was then explored by multiple linear regression [eqn (2)].

$$k_{obs} = k_{2(P1)}[H_2PO_4^-]_{50} + k_{2(P2)}[HPO_4^{2-}]_{50} + k_{2(OH)}[OH^-]_{50} + C \quad (2)$$

Both $[H_2PO_4^-]_{50}$ and $[OH^-]_{50}$ proved to be statistically insignificant, eqn (2) reducing to eqn (3):

$$k_{obs} = (1.017 \pm 0.202)[HPO_4^{2-}]_{50} + (0.0016 \pm 0.0008)\ r^2 = 0.9716 \quad (3)$$

where the uncertainties on $k_{2(P2)}$ and C are the 95% confidence intervals.

The pH-dependence of reaction rate is thus merely apparent, arising not from actual dependence on $[H^+]$ (or $[OH^-]$) but from the variation in $[HPO_4^{2-}]_{50}$ characteristic of the different buffers. The intercept of eqn (3) indicates the occurrence of reaction when there is no HPO_4^{2-} present. Since eqn (3) shows the reaction to be independent of $H_2PO_4^-$ (despite this being the buffering anion in the larger concentration) the intercept must be due to the low concentration of HPO_4^{2-} that arises *via* protolytic equilibrium with $H_2PO_4^-$. This is confirmed by the data of Table 6 that reports the variation in k_{obs} measured on solutions of KH_2PO_4 in 50% aqueous MeCN at constant ionic strength (0.1 mol dm^{-3}) in the absence of added HPO_4^{2-}. When these rate constants are plotted against $[H_2PO_4^-]_{50}$, the resultant graph has a gradient (0.0017 ± 0.0007) similar to the intercept of eqn (3), and no significant intercept itself. As the pH_{50} values of the solutions used for these measurements were constant at 5.57 within experimental error, the derived buffer ratio of 602.6 [*i.e.* antilog (8.35 − 5.57)] allows the equilibrium concentrations of HPO_4^{2-} arising from ionisation of $H_2PO_4^-$ to be evaluated. When k_{obs} is plotted as a function of such $[HPO_4^{2-}]_{50}$ (see Fig. 1, inset) the resultant graph has gradient (1.018 ± 0.403) (*i.e.* $k_{2(P2)}$/dm^3 mol^{-1} s^{-1}) in agreement with that of eqn (3) but without significant intercept. Combination of the two sets of data obtained at constant ionic strength (Fig. 1) permits the evaluation of $k_{2(P2)}$ with greater precision than from either set alone: $k_{2(P2)} = (1.02 \pm 0.13)$ dm^3 mol^{-1} s^{-1}.

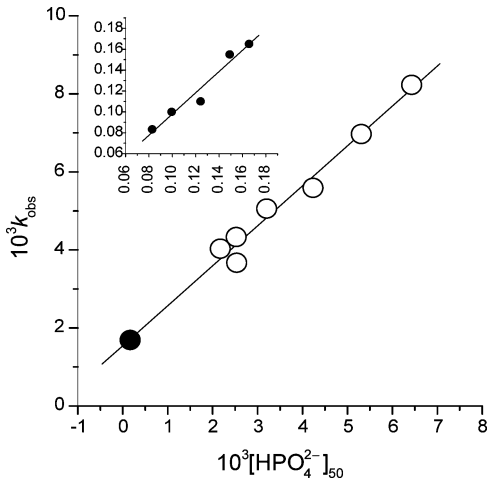

Fig. 1 Variation of k_{obs} with $[HPO_4^{2-}]_{50}$. Open circles: data for *added* HPO_4^{2-}; closed circle and inset: data for HPO_4^{2-} derived protolytically from $H_2PO_4^-$.

The results of this section thus confirm that HPO_4^{2-} is the sole kinetically active buffer component in the pH-range examined. The fact that the value of $k_{2(P2)}$ found here is less than that of (2.51 ± 0.48) dm^3 mol^{-1} s^{-1} given in (iv) (see Table 3, entry 10) for the same initial values of [**1**] and [**2**] is due to the difference in ionic strength between the two cases: 0.09 mol dm^{-3} here as compared to the intrinsic value of 0.04 mol dm^{-3} in (iv); a lower reaction rate at higher ionic strength is expected from the results in (v).

(vii) Dependence of reaction rate upon solvent composition

A limited set of experiments was performed in which the effect on reaction rate of variation in the proportions of MeCN to aqueous buffer was examined. Table 7 reports pseudo-first order rate constants k_{obs} and second order constants, $k_{2(Cu)V}$ (derived from the variation of k_{obs} with $[\mathbf{2}]_{init}$) for two solvents obtained by diluting an aqueous buffer ($B_{aq} = 0.05$ mol dm^{-3}) to the extents of 20% and 30% by volume, respectively, with MeCN; also given for comparison are the corresponding results for 50% dilution (*cf.* Table 2, column 4 and Table 3, entry 3).

As the effect on k_{obs} of variation in buffer concentration for each of the new solvent mixtures has not been investigated, we cannot derive either values of $k_{2(P2)}$ or values of third order constants as was

Table 6 Variation with concentration of dihydrogenphosphate at constant ionic strength[a] of the pseudo-first order rate constant for the reduction of 4-methoxybenzenediazonium ion by tetrakis(acetonitrile)copper(I)

B_{aq}/mol dm^{-3} [b]	$[KNO_3]_{aq}$/mol dm^{-3}	$[H_2PO_4^-]_{50}$/mol dm^{-3} [c]	$10^4[HPO_4^{2-}]_{50}$/mol dm^{-3} [c]	10^4k_{obs}/s^{-1} [d]
0.20	0.00	0.0998	1.657	1.65 ± 0.12
0.18	0.02	0.0899	1.491	1.55 ± 0.12
0.15	0.05	0.0749	1.243	1.10 ± 0.08
0.12	0.08	0.0599	0.994	1.00 ± 0.07
0.10	0.10	0.0499	0.828	0.83 ± 0.06

[a] The ionic strength, I_{aq}, of the initial aqueous solutions of KH_2PO_4 was adjusted to 0.20 mol dm^{-3} with KNO_3; I_{50} values were 0.10 mol dm^{-3}. [b] Concentration of aqueous KH_2PO_4. [c] Calculated from B_{50} (*i.e.* $0.5B_{aq}$) and $r_{B50} = 602.56$ [*i.e.* antilog (8.35 − 5.57)], see text. [d] Each value is the mean of duplicate determinations in which **1** (7.5×10^{-5} mol dm^{-3}) was reduced by **2** (1.489×10^{-3} mol dm^{-3}); the uncertainty is an arbitrary 7.5% of the value.

Table 7 Observed pseudo-first order rate constants ($10^3 k_{obs}/s^{-1}$) and derived second order and quasi-third order constants[a] for the reduction of 4-methoxybenzenediazonium ion[b] by tetrakis(acetonitrile)copper(I) in buffers of varied solvent composition

	Buffer		
	V:[d] 20%	30%	50%
	B_V:[e] 0.04 mol dm^{-3}	0.035 mol dm^{-3}	0.025 mol dm^{-3}
$10^4[\mathbf{2}]_{init}$/mol dm^{-3}[c]	pH_V:[f] 7.53	7.76	7.99
3.726	5.10 ± 0.49	3.15 ± 0.36	2.22 ± 0.24
7.505	10.18 ± 0.84	6.01 ± 0.41	6.61 ± 0.42
11.20	14.87 ± 0.53	9.18 ± 0.90	10.45 ± 1.80
14.89	19.74 ± 1.02	12.73 ± 0.72	13.68 ± 1.74
18.56	25.82 ± 2.15	16.62 ± 0.85	17.78 ± 1.20
$k_{2(Cu)V}$/dm^3 mol^{-1} s^{-1}:	13.75 ± 1.09	9.08 ± 1.10	10.31 ± 0.84
$l_{3(V)}$/dm^6 mol^{-2} s^{-1}:	807 ± 64	594 ± 72	1357 ± 111[g]

[a] Uncertainties in k_{obs} are the standard deviations of the set of measurements of each rate constant; uncertainties in $k_{2(Cu)V}$ and $l_{3(V)}$ are 95% confidence intervals. [b] Cuvette concentration 7.5×10^{-5} mol dm^{-3}. [c] Cuvette concentrations. [d] Percentage v/v of MeCN in buffer. [e] Total concentration of phosphate buffering salt. [f] Measured pH values. [g] *Cf.* the true third order constant, $k_{3(50)} = (1.81 \pm 0.13) \times 10^3$ dm^6 mol^{-2} s^{-1}.

done for the 50% aqueous MeCN mixture. However, quasi-third order constants, $l_{3(V)}$, may be calculated by division of the second order constants $k_{2(Cu)V}$ in Table 7 by $[HPO_4^{2-}]_V$, calculated *via* the buffer ratios from the values of B_V, pH_V (see header to Table 7) and pK_{aV} (Table 1), appropriate to the particular solvent mixture.[28] It may be seen that whereas $k_{2(Cu)20} > k_{2(Cu)50} > k_{2(Cu)30}$, allowance for the differences in $[HPO_4^{2-}]_V$ results in the order $l_{3(50)} > l_{3(20)} > l_{3(30)}$; neither the second order constant nor the quasi-third order constant decreases smoothly with the amount of MeCN in the mixed solvent. Several factors are relevant here: the pH_V of the aqueous acetonitrile buffers does not vary linearly with the mole-fraction of MeCN (unlike pK_{aV} and pK_{apV})[24a–c] with the result that, for the three solvent compositions examined, the difference between pK_{aV} and pH_V, and hence the buffer ratio, is least when V is 30%. This affects the relative values calculated for $[HPO_4^{2-}]$. Additionally, the viscosity η_{50} of 50% v/v aqueous MeCN (8.347×10^{-4} kg m^{-1} s^{-1}) is less than η_{30} and η_{20} (9.754×10^{-4} and 9.615×10^4 kg m^{-1} s^{-1}, respectively, see Table 1), the binary solvent mixture exhibiting a maximum in viscosity at *ca.* 20% v/v MeCN.[25] The relative permittivities, ε_{rV}, of the different solvent mixtures also differ (see Table 1) which is, no doubt, also significant for reactions between ionic species. We suggest it is the interplay of these several factors that determines the irregular ordering found for $k_{2(Cu)V}$ and $l_{3(V)}$.

Using stability constants from the literature,[20] the concentrations of the complexes $[Cu^I(NCMe)_n(OH_2)_{(4-n)}]^+$ (n, 1–3) present in each of the different solvent mixtures may be calculated for the range of [**2**] employed. The relative proportions of the complexes having n 3 and 2 are 91.1 : 8.8, 86.0 : 13.8 and 80.2 : 19.4, respectively, for V = 50, 30 and 20%. The complex $[Cu^I(NCMe)(OH_2)_3]^+$ is negligible in all three solvents amounting to less than 0.5% of total Cu(I) in all cases. For a particular percentage of MeCN, the relative proportions of the different complexes are invariant in the concentration ranges of Cu(I) employed; it is therefore impossible to extract rate constants for individual complexes; indeed, in each solvent mixture, the values of k_{obs} are correlated by the concentrations of any single complex with a squared correlation coefficient $r^2 \geq 0.995$. Any potential differences in the reactivities of individual complexes thus cannot be discerned in the irregular ordering of $k_{2(Cu)V}$ and $l_{3(V)}$.

(viii) Gasometric experiments

As already indicated, the reaction of interest may be monitored gasometrically.[29] In order to generate a volume of N_2 sufficient for measurement, the concentration of **1** under these conditions must necessarily be greater than when the reaction is monitored spectrophotometrically (0.01 mol dm^{-3} compared with 7.5×10^{-5} mol dm^{-3}) and convenient rates are obtained when the concentrations of **1** and **2** are similar. Experiments were run in which **1** was reduced in aqueous MeCN buffer (B_{50} = 0.025 mol dm^{-3}) by **2** in three different conditions of initial concentration, $([\mathbf{2}]/[\mathbf{1}])_{init}$, respectively: 0.02/0.01, 0.01/0.01 and 0.01/0.02. For each set of conditions, volumes of evolved N_2, v_t, were measured at 10 s intervals and converted to the percentage, $Q_{([\mathbf{2}]/[\mathbf{1}])}$, of the theoretically available millimolar volume at SATP

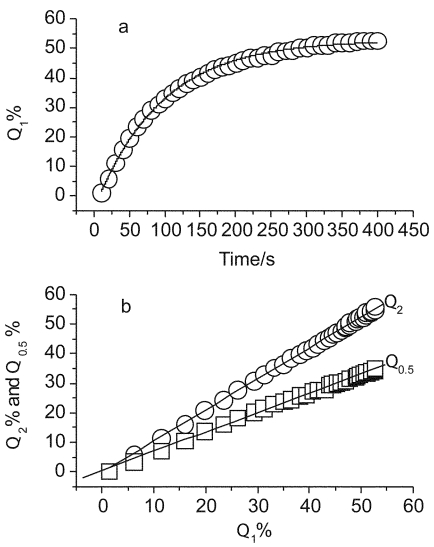

Fig. 2 **a** Variation with time of the volume percentage, Q_1, of N_2 at SATP evolved on reduction of **1** by **2** in a phosphate buffer in 50% aqueous MeCN (B_{50} = 0.025 mol dm^{-3}; [**1**] = [**2**] = 0.01 mol dm^{-3}). **b** Plots of Q_2 and $Q_{0.5}$ *versus* Q_1; for Q_2, B_{50} = 0.025 mol dm^{-3}, [**1**] = 0.01 mol dm^{-3} and [**2**] = 0.02 mol dm^{-3}; for $Q_{0.5}$, B_{50} = 0.025 mol dm^{-3}, [**1**] = 0.01 mol dm^{-3} and [**2**] = 0.005 mol dm^{-3}.

($v_m = 24.79$ cm^3; $2v_m$ for [**1**] = 0.02 mol dm^{-3}). Fig. 2a is a plot of Q_1 *versus* time; the curve is fitted by a first order expression [eqn (4)].

$$Q_1 = (57.28 \pm 2.20)\{1 - \exp[-10^{-2} \times (1.064 \pm 0.144)t]\} - (4.52 \pm 3.19)\ R^2 = 0.9996 \quad (4)$$

The spectrophotometric experiments have indicated the reaction to be of third order overall (first order in each of [**1**], [**2**] and [HPO_4^{2-}]), thus *second* order behaviour would be expected for experiments carried out in a particular buffer. Fig. 2b shows the plots of Q_2 and $Q_{0.5}$ *versus* Q_1; the linearity of these plots demonstrates that, at the higher reactant concentrations required for the gasometric experiments, the order with respect to Cu(I) falls to zero, the rate of evolution of N_2 being independent of [**2**] when this is varied by a factor of two on either side of equality with that of the diazonium ion. The mean value of the observed gasometric rate constant, $k_{obs}^{(g)}$, obtained from six runs (each of the three initial conditions in duplicate) was $(1.024 \pm 0.114) \times 10^{-2}$ s^{-1} where the uncertainty is twice the standard error on the mean (see ESI Tables S2(i) and S2(ii)‡). An experiment was also run for [**1**] = [**2**] = 0.01 mol dm^{-3} but in buffer: $B_{50} = 0.081$ mol dm^{-3} (see Discussion).

(ix) The product distribution

Product distribution data were obtained for three overlapping subsets of initial reactant concentrations: (a) $[\mathbf{1}]_{init} = 0.01$ mol dm^{-3}, variable $[\mathbf{2}]_{init}$; (b) $[\mathbf{2}]_{init} = 0.0577$ mol dm^{-3}, variable $[\mathbf{1}]_{init}$; (c) $[\mathbf{1}]_{init} = 0.08$ mol dm^{-3}, variable $[\mathbf{2}]_{init}$. The reactions of **1** with **2** in these various concentrations were carried out in 50 cm^3 volumes of 50% aqueous MeCN buffered by phosphate, $B_{50} = 0.081$ mol dm^{-3}, $pH_{50} = 7.92$ [see Experimental (vi)]. The reaction products methoxybenzene, **3**; 4,4′-dimethoxybiphenyl, **4**; 4,4′-dimethoxy-azobenzene, **5**; 4-methoxyphenol, **6**; 2-(4-methoxyphenyl)ethanonitrile, **7**; 4-methoxybenzonitrile, **8**; and 2,4′- and 3,4′-dimethoxybiphenyl, **9** and **10**, respectively, were identified by comparison of their mass spectra and retention times with those of authentic substances; trace amounts of 4-methoxyphenylethanone, **11**, were also occasionally observed.

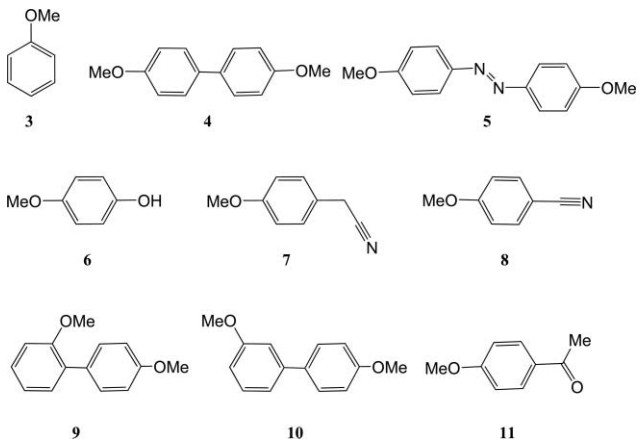

Products **3–5** are the expected 'Sandmeyer by-products' (see Introduction). Although phenols are known by-products of Sandmeyer reactions under hot synthetic conditions in which a reactant diazonium ion might undergo a degree of heterolysis, **6** was unexpected in this case since one of the reasons for choosing **1** as the substrate for investigation was on account of its thermal stability at 298 K over the duration of experiment.[14] Nor was the production of **6** *via* the trapping of 4-methoxyphenyl radicals by Cu^{2+} a likely route[1,7] as, initially, none of the latter is present and much of that formed in the reaction is precipitated as a phosphate salt. The nitriles **7** and **8** clearly must arise from the use of solvent containing MeCN.

Since the stoichiometry of the overall reaction of **1** with **2** to give the above products is unknown, it may be uncertain as to which particular reactant is yield-determining; theoretical percentage yields therefore cannot be found reliably. However, the composition of the mixture of organic products can be related to the fraction of the initial amount of **1** which is accountable as products, *i.e.* $[\Sigma(n \times m_n)]/m_{Dz}$ where m_n is the amount (mol) of an analysed product, n is the number of aromatic rings (1 or 2) that it contains and m_{Dz} is the initial amount of the diazonium ion, **1**, taken. The chromatograph was calibrated for quantitative analysis of **3–10** using authentic substances with dibenzofuran as internal standard. The chromatographic peak areas of products were converted into mol, m_n, by use of the internal standard: $m_n = F_r(A_n/A_s)m_s$ where A_n and A_s are, respectively, the peak areas of analyte and internal standard, m_s is the amount of the latter used (1×10^{-4} mol) and F_r is the appropriate response factor determined by prior calibration.

The amounts so obtained were converted into normalised percentage (%$_N$) yields *via* eqn (5):

$$P\%_N = [100(n \times m_n)/m_{Dz}]/\{[\Sigma(n \times m_n)]/m_{Dz}\} = 100(n \times m_n)/[\Sigma(n \times m_n)] \quad (5)$$

The composition of the product mixture is thus expressed in percentages of that amount of initial **1** which is accountable as observed products, due regard being taken of the number of molecules of **1** required for the formation of a molecule of each particular product. The normalised percentage distributions of the 5 main products are presented in Table 8 (see ESI, Table S3 for minor products **8**, **9** and **10** also‡).

In all conditions, the 'Sandmeyer by-products' **3–5** are the main constituents of the product mixture with the azoarene **5** predominating over the biaryl **4** as expected for a reactant diazonium ion bearing an electron-donating substituent.[2] The unexpected phenol **6** exhibits a somewhat variable occurrence but, in general, resembles **4** in quantity and distribution. By comparison, the nitrile **7** though occurring in each subset is relatively minor. The benzonitrile, **8**, does not occur significantly in subset (a). The asymmetrical biaryls **9** and **10** are very minor and their occurrence is limited to conditions in which [**1**] is relatively high but the ratio $([\mathbf{2}]/[\mathbf{1}])_{init}$ is low; whenever they occur, the yield of the 3,4′-isomer exceeds that of the 2,4′-isomer.

Synthetically useful hydrodediazoniation reactions normally involve homolysis of the diazonium ion, often induced by Cu(I), to produce an aryl radical which then abstracts a hydrogen atom from a suitable donor.[30] Such a process occurring adventitiously as a side-reaction during Sandmeyer procedures, especially those which employ mixed solvents, could account for the occurrence of the reduction product ArH as a by-product. However, reduction products are reported as by-products in Pschorr cyclisations (which lack the efficiently transferred Cu-halide/cyanide ligands of Sandmeyer reactions) in aqueous conditions and in the absence of homolytic H-donors.[31] This suggests that ArH might also arise from the protonolysis of organocopper intermediates.

Table 8 Normalised percentage distribution of main reaction products[a]

Entry	$([\mathbf{2}]/[\mathbf{1}])_{init}$	Acc Dz[b]	AnH, **3**	An–An, **4**	AnN=NAn, **5**	AnOH, **6**	$AnCH_2CN$, **7**
Subset (*a*): $[\mathbf{1}]_{init}$, 0.01 mol dm^{-3}							
1	0.193	4.94	29.78	0.00	70.22	0.00	0.00
2	0.371	11.68	60.49	4.46	33.56	0.00	1.50
3	0.922	48.85	46.85	6.73	26.53	8.40	6.08
4	1.872	78.02	22.13	8.78	54.29	13.31	1.49
5	5.925	91.54	9.83	7.86	73.21	8.71	0.40
6	9.248	93.31	4.90	3.95	86.14	5.01	0.00
Subset (*b*): $[\mathbf{2}]_{init}$, 0.0577 mol dm^{-3}							
7	0.577	32.81	40.91	16.25	20.56	13.22	2.06
8	0.722	37.24	48.77	14.44	19.50	9.14	0.89
9	1.435	76.79	40.74	13.10	30.19	9.74	0.73
5	5.925	91.54	9.83	7.86	73.21	8.71	0.40
10	12.13	94.12	3.46	4.05	86.10	6.39	0.00
Subset (*c*): $[\mathbf{1}]_{init}$, 0.08 mol dm^{-3}							
11	0.024	1.71	26.88	9.86	60.97	0.00	0.00
12	0.048	3.57	36.74	10.52	36.89	0.00	3.58
13	0.120	9.93	41.76	13.24	24.40	0.00	12.3
8	0.722	37.24	48.77	14.44	19.5	9.14	0.89

[a] An is 4-methoxyphenyl. [b] Percentage accountability of **1**, as products, *i.e.* $100 \times [\Sigma(n \times m_n)]/m_{Dz}$ (see text).

Table 9 The extent of isotopic labelling of 4-methoxybenzene, **3**, formed in phosphate-buffered 50% v/v MeCN in D_2O for various initial concentrations of reactants

Entry	$[\mathbf{1}]_{init}$/mol dm^{-3}	$[\mathbf{2}]_{init}$/mol dm^{-3}	$([\mathbf{2}]/[\mathbf{1}])_{init}$	A_H/A_D[a]
1	0.0107	0.0039	0.364	15.5
2	0.0097	0.0096	0.990	2.85
3	0.0102	0.0577	5.657	0.85
4	0.0786	0.0577	0.734	0.41

[a] Ratio of integrated mass spectral peak areas at $m/z = 108$ and 109, the latter being corrected for content of ^{13}C, ^{17}O and ^{2}H at natural abundance.

In order to test this possibility, experiments were carried out using a phosphate buffer made up in 50% v/v MeCN in D_2O ($B_{50} = 0.08$ mol dm^{-3}) in the expectation that **3** formed by H-abstraction would not be isotopically labelled whereas that formed by deuteronolysis of any organocopper intermediates would be so labelled. From the extent of labelling, an indication of the degree to which, in aqueous MeCN, H-abstraction and protonolysis pathways contribute to the yield of **3** might be inferred. The results are given in Table 9. An isotope effect is clearly evident which shows that, according to conditions, either unlabelled or labelled **3** can predominate.

Discussion

(i) The rate-determining step

The spectrophotometric kinetic measurements described above [Results (iv), (vi)] have shown that when the reduction of 4-methoxybenzenediazonium ion, **1**, by the complexes derived from $[Cu^I(NCMe)_4]^+$, **2**, in phosphate-buffered 50% v/v aqueous MeCN is monitored by the disappearance of **1**, the reaction is of third order overall, being of first order in each of [**1**], [**2**] and $[HPO_4^{2-}]$. By contrast, the gasometric experiments which monitored the evolution of N_2 during the reduction [Results (viii)] exhibited no dependence on [**2**].

In general, if reactants X and Y associate reversibly (with k_a and k_{-a}, respectively, as forward and backward rate constants) to form an adduct, A, which then reacts with reactant Z (with rate constant k_r) to give a product, P, a routine application of the steady state approximation to A gives eqn (6) for the rate of disappearance of X or appearance of P:

$$-d[X]/dt = d[P]/dt = k_a k_r[X][Y][Z]/(k_{-a} + k_r[Z]) \quad (6)$$

In the instance that $k_r[Z] \ll k_{-a}$, eqn (6) approximates to eqn (7):

$$-d[X]/dt = d[P]/dt = (k_a k_r/k_{-a})\,[X][Y][Z] \quad (7)$$

i.e. third order behaviour is observed for the disappearance of X. If, however, $k_{-a} \ll k_r[Z]$, eqn (6) approximates to eqn (8) in which the reaction shows no dependence on Z and k_a is identified as the overall rate-determining rate constant.

$$-d[X]/dt = d[P]/dt = k_a[X][Y] \quad (8)$$

Allowing that each molecule of X which reacts in the rate-determining step gives rise to a molecule of P, then $[X]_0 = [P]_\infty$ where $[X]_0$ is the initial concentration of X and $[P]_\infty$ is the final concentration of P, eqn (8) may be recast as eqn (9) if [Y] is effectively constant:

$$d[P]/dt = k_a([P]_\infty - [P])[Y] = k_a'([P]_\infty - [P]) \quad (9)$$

Separation of variables and integration followed by rearrangement gives eqn (10):

$$[P] = [P]_\infty\{1 - \exp(-k_a' t)\} \quad (10)$$

These general circumstances correspond to our observations if X is identified with **1**, Z with **2**, Y with HPO_4^{2-} and P with N_2. The inference that the rate-determining step involves the addition of HPO_4^{2-} to **1** is consistent with the finding [Results (v)] that the product of the charges of the ions reacting in the rate-determining step, $z_i z_j$, is −2. Eqn (10) has the same algebraic form as eqn (4), the extra term in the latter arising in the non-linear curve-fitting from uncertainty in the experimental onset of reaction due to the time required for the mixing of reactants and the generation of

sufficient N_2 for response of the gas-cell. In eqn (4) the yield of N_2 is quoted as a percentage of the maximum theoretically possible rather than as a concentration as in eqn (10). However, since the unit of measurement of quantity is immaterial for a first order reaction, $k_{obs}{}^{(g)}$ in eqn (4) can be identified with k_a' in eqn (10). The latter was defined as $k_a[Y]$, *i.e.* $k_a[HPO_4^{2-}]$. In these experiments the total buffer concentration, B_{50}, was 0.025 mol dm^{-3} hence $[HPO_4^{2-}]$ was 7.6×10^{-3} mol dm^{-3}; the gasometric rate-determining second order rate constant, k_a, is therefore given by $k_a = (1.024 \pm 0.114) \times 10^{-2}$ s^{-1}/7.60×10^{-3} mol dm^{-3} $= (1.4 \pm 0.15)$ dm^3 mol^{-1} s^{-1}.

The finding that Q_∞ is evaluated at 57.3% and not 100% (within an experimental error of ~10%[32]) occurs because our observations are not, in reality, made on a system where the decrease in [**1**] depends simply on its participation in the rate-determining step. There are rapid steps that follow upon the rate-determining step and which result in the removal of **1** from the system without loss of N_2, as evidenced by the formation of the azobenzene, **5**. Reduction of **1** results in the formation of the 4-methoxyphenyl radical; however, in the relatively concentrated conditions of the gasometric experiments the probability of this radical reacting with **1** or **2** (reactions leading to **5**, *vide infra*) is greater than under the dilute spectrophotometric conditions where H-abstraction from MeCN is more likely. For the complex system under investigation, therefore, a true value of the ratio k_r/k_{-a} cannot be inferred from the value of the third order rate constant determined spectrophotometrically and the second order constant k_a evaluated gasometrically.

(ii) Mechanism of reduction

The direct reduction of **1** by **2**, or derived cations $[Cu^I(NCMe)_n(OH_2)_{(4-n)}]^+$, ($n$, 1–3), is evidently prevented by a combination of adverse reduction potentials and the coulombic repulsion between cationic reactants. However, the addition of HPO_4^{2-} to **1** will produce a mono-anionic adduct (A^-) and, though this hard phosphate-derived anion is not expected to be a strong ligand for a soft Cu(I) cation, it should, on account of coulombic attraction, be able to displace a neutral water ligand from a hydrated ion derived from **2** hence bridging the diazonium and metal centres in an overall neutral precursor complex or transition state (T) (Scheme 2). The formation of the adduct A^- changes the geometry of the CNN moiety from linear in the ion[33] to a bent configuration as in the radical[34] and so assists in overcoming the high inner-sphere reorganisation energy-barrier

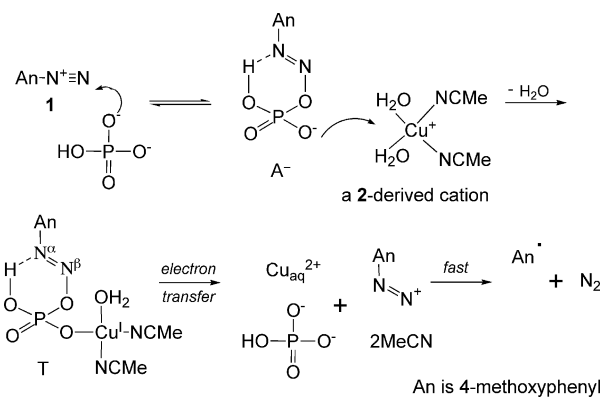

Scheme 2

to electron transfer.[35] Speculatively, in Scheme 2, a *trans*-addition of HPO_4^{2-} to **1** is shown, resembling that of ascorbate;[36] [in the Scheme and henceforth, An ≡ 4-methoxyphenyl (anisyl)]. The hydrogen-bond to N_α possible as a result of *trans*-addition should stabilise enthalpically the formation of A^- and may facilitate the orientation of orbitals necessary for electron transfer by limiting the torsional freedom of T. We suggest an electron transfer *via* the σ-framework in T on account of the contracted nature of the d-orbitals on copper.

(iii) Mechanisms of product formation

Reactions of 4-methoxyphenyl radical, An•, with organic molecules. Likely pathways to several observed products can be inferred from the elementary reactions expected of An•. One such reaction is H-abstraction from MeCN in the mixed solvent to give **3** (and $NCCH_2$•); rate constants for H-abstraction from MeCN by other aryl radicals are known and will serve as useful references in the simulation to follow.[37,38] A second type of anticipated elementary reaction is addition to unsaturated molecules. Radicals can add to diazonium ions either at N_β or at unsubstituted ring positions.[39,40] The addition of An• to N_β of **1** produces the cation radical of 4,4′-dimethoxyazobenzene which, on reduction by Cu(I) would give **5**; rate constants are known for additions of aryl radicals to diazonium functions.[40,41] Addition of An• at ring-positions 2 and 3 of **1** affords routes to both observed minor asymmetrical biaryls **9** and **10** (Scheme 3). The diazonio-cyclohexadienyl radicals **12** and **13** resulting from such addition require no oxidant for aromatisation. Both may be deprotonated to give biaryldiazenyl radicals which would rapidly lose N_2 producing biaryl radicals; these would then abstract hydrogen from MeCN to give **9** and **10** with concomitant $NCCH_2$•. The predominance of **10** over **9** is consistent with the fact that ring-substituents of –M character activate adjacent positions to homolytic arylation better than +M substituents:[42] the directing influence of $-N_2^+$ on An• in its attack on **1** thus outweighs that of –OMe.

Addition of An• to MeCN provides a route to the observed minor product AnCN, **8**.

$$An^{\bullet} + MeCN \rightarrow An(Me)C{=}N^{\bullet} \rightarrow \mathbf{8} + Me^{\bullet}$$

If these reactions were to be reversible, the equilibria would be expected to lie to the right on account of the gain in conjugation. The trace product 4-methoxyphenylethanone, **11**, also derives from the intermediate iminyl radical:

$$An(Me)C{=}N^{\bullet} + MeCN \rightarrow An(Me)C{=}NH + NCCH_2^{\bullet}$$

$$An(Me)C{=}NH + H_2O \rightarrow \mathbf{11} + NH_3$$

Reactions of organocopper intermediates. Aliphatic radicals are well known to react rapidly with Cu^+_{aq} to produce Cu(II) adducts[8–12] and the same is expected for An• reacting with the cations arising from **2** in aqueous MeCN:[43]

$$An^{\bullet} + [Cu^I(NCMe)_n(OH_2)_{(4-n)}]^+ \rightarrow (Cu^{II}An)^+_{aq} + n\text{MeCN}$$

It is likely that MeCN ligands on Cu^+ will be lost on the change in oxidation state but that ligation by water will be retained.

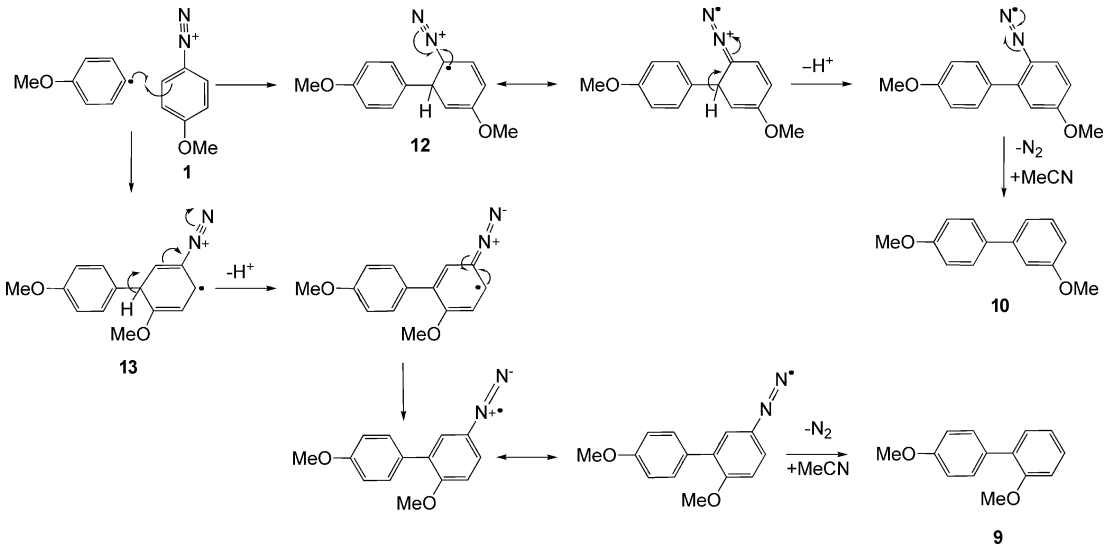

Scheme 3

Behaviour similar to that of An$^{\bullet}$ is expected for $NCCH_2^{\bullet}$:

$$NCCH_2^{\bullet} + [Cu^{I}(NCMe)_n(OH_2)_{(4-n)}]^+ \rightarrow (Cu^{II}CH_2CN)^+_{aq} + n\text{MeCN}$$

$(Cu^{II}An)^+_{aq}$ and $(Cu^{II}CH_2CN)^+_{aq}$ are thus the expected primary organocopper intermediates. Aliphatic organocopper(II) species are known to undergo protonolysis in water.[8c,11] However, if these primary intermediates are to enter into other reactions which lead to observed products, their protonolyses must be slow in comparison with their other reactions. Inspection of entries 3–10 of Table 8 shows that as $([\mathbf{2}]/[\mathbf{1}])_{init}$ is increased the normalised percentage yield of the azoarene, **5**, increases at the expense of all other products. Since the formation of $(Cu^{II}An)^+_{aq}$ competes with the formation of **5** *via* addition of An$^{\bullet}$ to **1**, the yield of **5** by this latter route will decrease as $[\mathbf{2}]/[\mathbf{1}]_{init}$ is increased. There must therefore exist an additional route to **5** that involves $(Cu^{II}An)^+_{aq}$.

Symmetrical biaryls constitute a major Sandmeyer by-product (see Introduction). Their formation by the combination of aryl radicals can be excluded immediately as aryl radicals are highly reactive species which are too rapidly consumed in reactions with abundant non-radical species for there to be significant probability of such radical–radical encounter. Organocopper intermediates are thought to be involved: Cohen and co-workers[5] suggested Cu(II) and Cu(III) intermediates in a sequence terminating in the reductive elimination of biaryl from the latter:

$$Ar^{\bullet} + Cu(I) \rightarrow (Cu^{II}Ar)^+$$

$$Ar^{\bullet} + (Cu^{II}Ar)^+ \rightarrow (Cu^{III}Ar_2)^+$$

$$(Cu^{III}Ar_2)^+ \rightarrow Ar\text{–}Ar + Cu(I)$$

Meyerstein and co-workers[11] have observed that the decomposition of $(Cu^{II}Me)^+$ follows a second order rate law to give ethane: $2(Cu^{II}Me)^+ \rightarrow C_2H_6 + 2Cu^+$, and other aliphatic organocopper(II) species behave similarly. Furthermore, it is known that Cu^{2+}_{aq} and certain Cu(II) complexes oxidise CN^- to give cyanogen, NC–CN, in a process which is also of second order in Cu(II), the reductive elimination of cyanogen from a binuclear intermediate being rate-determining.[44]

$$2Cu^{2+} + 6CN^- \rightleftharpoons [Cu^{II}{}_2(CN)_6]^{2-}$$

$$[Cu^{II}{}_2(CN)_6]^{2-} \rightarrow NC\text{–}CN + 2[Cu^{I}(CN)_2]^-$$

In the light of these observations and leaving aside for the moment detail of the specific mechanism, a self-reaction of $(Cu^{II}An)^+_{aq}$ is tentatively suggested as a route to **4**.[45]

$$2(Cu^{II}An)^+_{aq} \rightarrow \mathbf{4} + 2Cu(I)$$

On this assumption, the fact that the yield of **5** increases at the expense of that of **4** as $([\mathbf{2}]/[\mathbf{1}])_{init}$ is increased indicates that the reaction producing **5** depletes the availability of $(Cu^{II}An)^+_{aq}$. Reduction of $(Cu^{II}An)^+_{aq}$ provides an explanation:

$$(Cu^{II}An)^+_{aq} + [Cu^{I}(NCMe)_n(OH_2)_{(4-n)}]^+ \rightarrow (Cu^{I}An) + Cu^{2+}_{aq} + n\text{MeCN} \quad (11)$$

$$(Cu^{I}An) + \mathbf{1} + n\text{MeCN} \rightarrow \mathbf{5} + [Cu^{I}(NCMe)_n(OH_2)_{(4-n)}]^+$$

Net reaction: $(Cu^{II}An)^+_{aq} + \mathbf{1} \rightarrow \mathbf{5} + Cu^{2+}_{aq}$

Essentially, complexes derived from **2** catalyse the addition of $(Cu^{II}An)^+_{aq}$ to **1** by converting it into the more strongly nucleophilic $(Cu^{I}An)$. The state of ligation of $(Cu^{I}An)$ is uncertain; $(Cu^{I}Ph)$ has been reported to be highly sensitive to moisture but to be stabilised against protonolysis on ligation by pyridine.[46] Ligation of $(Cu^{I}An)$ by MeCN could afford comparable stabilisation and hence facilitate its reaction with **1**.

For the production of 4-methoxyphenol, **6**, we have excluded both the thermolysis of **1** and the hydrolysis of $(Cu^{III}An)^{2+}$ formed by simple addition of An$^{\bullet}$ to Cu^{2+} [Results (ix)].[47] Nevertheless, an alternative involvement of Cu(III) is needed as the precursor to **6** since both organocopper(I)[46] and organocopper(II)[11] species undergo protonolysis not hydrolysis on reaction with water. First,

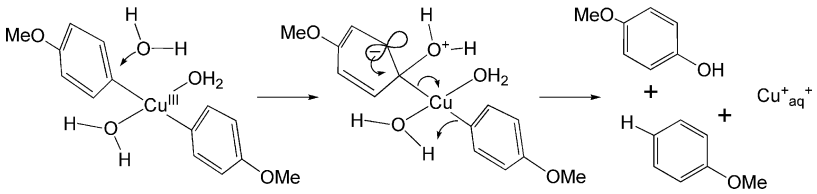

Scheme 4

we considered a caged reaction in which the MeCN and HPO_4^{2-} liberated on fragmentation of T (see Scheme 2) are ignored:

$$A^- + Cu(I) \rightarrow T \rightarrow |AnN_2^{\bullet} + Cu^{2+}{}_{aq}|_{cage\ 1} \rightarrow |N_2 + An^{\bullet} + Cu^{2+}{}_{aq}|_{cage\ 2} \rightarrow N_2 + (Cu^{III}An)^{2+}$$

$$(Cu^{III}An)^{2+} + H_2O \rightarrow \mathbf{6} + H^+ + Cu(I)$$

Assuming the rapid hydrolysis of $(Cu^{III}An)^{2+}$, this hypothesis requires that the ratio of **6** to the combined non-phenolic products should depend on $k_{add}/(k_{esc1} + k_{esc2})$ where k_{add} is the rate constant for *caged addition* of An$^{\bullet}$ to $Cu^{2+}{}_{aq}$ (in cage 2) and k_{esc1} and k_{esc2} are the rate constants for the escape of $AnN_2^{\bullet}$ and An$^{\bullet}$ radicals from their respective solvent cages; all three constants are of first order. Hence the prediction of the hypothesis is that the normalised percentage yield of **6** should be essentially constant irrespective of the conditions of experiment. Table 8 shows that this is not the case: as $([\mathbf{2}]/[\mathbf{1}])_{init}$ is increased, in subset (a) the normalised yield of **6** increases from zero to a maximum and then decreases; in subset (b) it starts at a high value and declines; in subset (c) only entry 8 cites any **6**. Formation of **6** *via* a caged reaction must therefore be rejected. (Since Cu^{2+} was precipitated as a phosphate salt in the product-study experiments, it is possible that the ions Cu^{2+} and HPO_4^{2-} would pair in cage 1 on their formation by electron transfer in T and thereby obviate reaction of An$^{\bullet}$ with Cu^{2+} in cage 2.)

In subsets (a) and (b) the trends in the yield of **6** are similar to those of **4** so we considered self-reactions of $(AnCu^{II})^+$ that might give rise to organocopper(III) species and thence **6**.

Simple disproportionation: $2(Cu^{II}An)^+{}_{aq} \rightarrow (Cu^{III}An)^{2+} + (Cu^{I}An)$

$$(Cu^{III}An)^{2+} + H_2O \rightarrow \mathbf{6} + Cu^+ + H^+$$

Disproportionation with aryl transfer: $2(Cu^{II}An)^+{}_{aq} \rightarrow (Cu^{III}An_2)^+ + Cu^+$ $(Cu^{III}An_2)^+ + H_2O \rightarrow \mathbf{6} + (Cu^{I}An) + H^+$

The complex $(Cu^{III}An)^{2+}$ is the congener of those formed on addition of aryl radicals to $Cu^{2+}{}_{aq}$[1] whereas $(Cu^{III}An_2)^+$ is the analogue of those proposed by Cohen[5] to arise from the addition of aryl radicals to $(Cu^{II}Ar)^+$. The two disproportionation sequences have the same net result:

$$2(Cu^{II}An)^+{}_{aq} + H_2O \rightarrow \mathbf{6} + (Cu^{I}An) + Cu^+ + H^+ \qquad (12)$$

Although not reported for aliphatic systems, disproportionation does not seem an unreasonable suggestion as $(Cu^{II}An)^+$ is an odd-electron species. In modelling the product distribution, we opted for disproportionation with aryl transfer for two reasons. First, it permits the reductive elimination of **4** from the mononuclear complex $(Cu^{III}An_2)^+$ as suggested by Cohen and co-workers,[5] although our immediate precursors to $(Cu^{III}An_2)^+$ differ from theirs. The more important second reason stems from the fact that hydrolysis of the Cu(III) intermediate, with or without aryl transfer, also produces an amount of $(Cu^{I}An)$ equal to that of **6** [reaction (12)]. If this is added to the $(Cu^{I}An)$ produced in reaction (11) the simulated distribution of **5** is not satisfactory for $([\mathbf{2}]/[\mathbf{1}])_{init} < 2$ in subset (a). [Modelling of subset (a) where [**1**] is low and the experimental data set largest was addressed before that of the other subsets; see below.] A satisfactory simulation of the distribution of **5** is possible, however, if the $(Cu^{I}An)$ arising from disproportionation undergoes protonolysis rather than addition to **1**. As there is no obvious way of distinguishing two $(Cu^{I}Ar)$ species with different reactivities, the difficulty is circumvented by adopting a concerted hydrolysis and protonolysis of the two An ligands of $(Cu^{III}An_2)^+$ without involvement of free $(Cu^{I}An)$ (Scheme 4):

$$(Cu^{III}An_2)^+ + H_2O \rightarrow \mathbf{6} + \mathbf{3} + Cu^+$$

Support for this tentative suggestion is the report[12] (based on measurements of activation volumes) that the hydrolysis of Cu^{III}–C bonds occurs by nucleophilic attack of a solvent water molecule at C whereas the protonolysis of a Cu^{II}–C bond occurs *via* a four-centred transition state comprising the Cu and C atoms together with the O and one H atom of a *cis*-aqua ligand. It is tempting to speculate further and suggest that $(Cu^{III}An_2)^+$, being a d^8 complex, is square-planar and exists in *cis*- and *trans*-forms as carbon ligands occupy a relatively high position in the spectrochemical series.[48] Reductive elimination of **4** could then occur from the former whilst the concerted reaction could occur in the latter as shown in Scheme 4.

By analogy with the self-reactions of $(Cu^{II}An)^+{}_{aq}$ suggested above, organocopper(III) species might also arise from the reaction of both primary organocopper(II) complexes and give observed products:

Ligand transfer: $(Cu^{II}An)^+{}_{aq} + (Cu^{II}CH_2CN)^+{}_{aq} \rightarrow \{Cu^{III}An(CH_2CN)\}^+ + Cu^+$

Reductive elimination: $\{Cu^{III}An(CH_2CN)\}^+ \rightarrow \mathbf{7} + Cu^+$

Concerted hydrolysis & protonolysis: $\{Cu^{III}An(CH_2CN)\}^+ + H_2O \rightarrow \mathbf{6} + MeCN + Cu^+$

and $\{Cu^{III}An(CH_2CN)\}^+ + H_2O \rightarrow \mathbf{3} + NCCH_2OH + Cu^+$

(iv) Computer simulation of the product distribution

Limitations of the model. The modelling program available, *Simula*,[49] is limited to 30 species and 30 reactions. As such it is inadequate for the simultaneous modelling of reactions to give all eight reaction products **3–10** if alternative pathways to individual products are to be distinguished and different potential intermediates specified. The simulation to be presented therefore excludes the minor asymmetrical biaryls **9** and **10** and

4-methoxybenzonitrile, **8**; comment will be made later on these exclusions. Various schemes were found which reproduced general trends in the product distributions reported in Table 8 but that presented in Scheme 5, though not a rigorously optimised fit of the data, was the most satisfactory. The reactions of Scheme 5 will be explained and discussed in this section. Reaction numbers cited here, without parenthesis, are specific to the Scheme and do not relate to earlier numbering. Initially, the loss of HPO_4^{2-} by precipitation of the Cu^{2+} salt was not considered but this aspect was introduced in a second stage.

Allocation of rate constants. Rate constants were assigned to reactions in the Scheme in three ways: by comparison with precedents when possible; others were assigned sufficiently large arbitrary values when not crucial, and the remainder were found by trial and error.

Reactions 1 and 2 concern the phosphate-buffered 50% v/v aqueous MeCN solvent. The pK_a of $H_2PO_4^-$ in this medium, pK_{a50}, is 8.35 (Table 1), hence $K_a = 4.5 \times 10^{-9}$. Assuming for the protonation of HPO_4^{2-} a rate constant of $k_{-1} = 1 \times 10^{11}$ dm^3 mol^{-1} s^{-1}, the value of 4.5×10^2 s^{-1} for k_1 follows from the value of K_a. Similarly, the autoprotolysis constant for the mixed solvent pK_{ap50} is 15.48 (Table 1) whence $1/K_{ap50} = 3.0 \times 10^{15}$. Assuming a rate constant of $k_2 = 3 \times 10^{11}$ dm^3 mol^{-1} s^{-1} for proton transfer from H_3O^+ to OH^- results in $k_{-2} = 1.0 \times 10^{-4}$ s^{-1}. The precedent for the assumed rate constants of the order of 10^{11} is that for proton transfer from H_3O^+ to OH^- in water (1.4×10^{11} dm^3 mol^{-1} s^{-1}).[50] Unit activity for water is implicit in the definition of the pK values used here (its formal concentration in the mixed solvent was 27.7 mol dm^{-3}).

Since the reactant concentrations in the study of the product distribution were comparable to those of the gasometric experiments, k_3 was set as 1.4 dm^3 mol^{-1} s^{-1} [*cf.* k_a in (i) above]; k_{-3} was set arbitrarily as 10 s^{-1} ensuring the equilibrium forming the adduct A^- lies to the left, and so consistent with the presence of phosphate having negligible effect on the UV spectrum of AnN_2^+ (*i.e.* **1**) in solution. The reduction step, reaction 4 was assigned a rate constant, $k_4 = 1.8 \times 10^3$ dm^3 mol^{-1} s^{-1}. Since a magnitude for k_4/k_{-3} could not be inferred from the kinetic measurements [*cf.* k_r/k_{-a} in (i) above], variations in the relative magnitudes of k_{-3} and k_4 were explored and assessed for their effects on the simulated evolution of N_2 in comparison with that observed experimentally; the stated values are those which gave the best outcome (see below). Scheme 5 excludes the species T shown in Scheme 2 but this is unimportant if it is formed and fragmented irreversibly. The rate constant for the fragmentation of $AnN_2^{\bullet}$, k_5, was set at 1×10^6 s^{-1}. Becker and co-workers[51] found a value of 1.5×10^6 s^{-1} for this reaction in 50% v/v aqueous *t*-BuOH. Again, since the radical is formed and fragmented irreversibly, the value used is immaterial provided it is sufficiently large.

Reactions 6–9 concern the key reactions of An$^{\bullet}$ produced by fragmentation of $AnN_2^{\bullet}$. Previously, by using the 2-benzoylphenyl radical as a radical clock, we have measured a rate constant of 1.2×10^5 dm^3 mol^{-1} s^{-1} for the abstraction of hydrogen by an aryl radical from MeCN in water,[37] a value in good agreement with that of Scaiano and Stewart[38] (1.0×10^5 dm^3 mol^{-1} s^{-1}) for H-abstraction by phenyl radical from MeCN in Freon. Since, in H-abstraction, phenyl radicals exhibit slightly electrophilic character,[52] in Scheme 5 we have assigned An$^{\bullet}$ an H-abstraction rate constant, k_6, of 5×10^4 dm^3 mol^{-1} s^{-1} as the electron-donating 4-MeO substituent is expected to reduce its electrophilicity somewhat relative to these comparators. The concentration of MeCN in the 50% v/v aqueous solvent (9.57 mol dm^{-3}) was used with this second order constant. The product AnH (*i.e.* **3**) formed in reaction 6 is labelled (*1*) to distinguish it from that formed by protonolysis of organocopper intermediates (see below).

In reaction 7, the ambiphilic An$^{\bullet}$ radical reacts nucleophilically on addition to the electron-deficient N_β of AnN_2^+;[53] one precedent for this reaction is the addition of 4-methylphenyl radical, 4-MePh$^{\bullet}$, to 4-$MeC_6H_4N_2^+$ for which Packer and co-workers[41b] measured a rate constant of 2×10^6 dm^3 mol^{-1} s^{-1}; another precedent is provided by Minisci and co-workers[40] who inferred a rate constant $\sim 10^6$ dm^3 mol^{-1} s^{-1} for the addition of 4-ClPh$^{\bullet}$ to 4-$ClC_6H_4N_2^+$; we accordingly ascribe k_7 a value of 3.0×10^7 dm^3 mol^{-1} s^{-1} to reflect the relatively greater nucleophilic character of An$^{\bullet}$ in comparison to 4-MePh$^{\bullet}$ and 4-ClPh$^{\bullet}$. Reaction 7 is shown as reversible: Bargon and Seifert[54] proposed reversibility of the addition of Ph$^{\bullet}$ to PhN_2^+ to explain scrambling of ^{15}N labelling in the latter and various CIDNP phenomena but, in the light of their pulse radiolysis studies, Packer and co-workers[41a] limited the rate constant for the dissociation of the radical cation of 4,4′-dimethylazobenzene to <10 s^{-1}. There is uncertainty as to whether the azobenzene radical cation itself exists in a σ- or π-state in fluid solution.[55] The electron-donating substitution in AnN=NAn$^{+\bullet}$ would stabilise it as a cation in either case, especially a conjugated π-state; accordingly, we set k_{-7} to 1 s^{-1}. It is envisaged that AnN=NAn$^{+\bullet}$ will be reduced irreversibly to AnN=NAn (*i.e.* **5**) by Cu(I); setting k_8 to 3.5×10^3 dm^3 mol^{-1} s^{-1} ensures that residual AnN=NAn$^{+\bullet}$ is normally negligible at the completion of reaction (but see later). AnN=NAn formed by reaction 8 is labelled (*1*) to distinguish it from that derived *via* the organocopper route (see below).

Methyl radical, Me$^{\bullet}$, reacts with Cu^+_{aq} to produce $(Cu^{II}Me)^+$ at a rate approaching the diffusion-controlled limit ($k = 3.5 \times 10^9$ dm^3 mol^{-1} s^{-1}).[11b] The change from Cu(I) to Cu(II) imputes electrophilic character to the radical in this process. The gas phase phenyl radical, Ph$^{\bullet(g)}$, has a higher electron affinity than Me$^{\bullet(g)}$ (1.096 eV compared to 0.080 eV)[56] hence aryl radicals such as An$^{\bullet}$ would be expected to react in solution with Cu^+_{aq} at, or close to, the diffusion-controlled limit. In the system under investigation, however, the Cu^+ is stabilised by up to three MeCN ligands which are expected significantly to increase the reduction potential from that of Cu^{2+}_{aq}/Cu^+_{aq} [see Results (ii)];[22] such an increase will cause a lowering in the expected reaction rate relative to Cu^+_{aq}. We therefore assign to k_9 a value of 7.5×10^8 dm^3 mol^{-1}, reflecting this reasoning. From the kinetic behaviour of their system, Cohen and co-workers[5] inferred the addition of 4-nitrophenyl radical, 4-$O_2NPh^{\bullet}$, to **2** in moist acetone to be reversible. We allowed this possibility for reaction 9 and arbitrarily assigned $k_{-9} = 5$ s^{-1}. Reaction 10 is that between Cu(I) and $NCCH_2^{\bullet}$ produced in reaction 6; following similar reasoning to that made for reaction 9, we assign k_{10} a value of 5×10^8 dm^3 mol^{-1}, somewhat lower than the value of 2.8×10^9 dm^3 mol^{-1} found for the electronically comparable $HO_2CCH_2^{\bullet}$ reacting with Cu^+_{aq}.[11b] Since addition of alkyl radicals to Cu^+_{aq} is not reversible in the absence of other factors such as stabilisation of the radical by an α-hydroxyl group[9] or conjugation[57] or hindering multidentate ligation of the metal,[11b] reaction 10 has not been made reversible.

Reaction	Reactants[a]		Products[a]	Rate constant[b]	
1	$H_2PO_4^-$	$\rightleftharpoons$	$HPO_4^{2-} + H_3O^+$	k_1	4.5×10^2
				k_{-1}	1.0×10^{11}
2	$H_3O^+ + OH^-$	$\rightleftharpoons$	H_2O	k_2	3.0×10^{11}
				k_{-2}	1.0×10^{-4}
3[c]	$AnN_2^+ + HPO_4^{2-}$	$\rightleftharpoons$	A^-	k_3	1.4
				k_{-3}	1.0×10^1
4[c]	$A^- + Cu^+$	$\rightarrow$	$AnN_2\cdot + Cu^{2+} + HPO_4^{2-}$	k_4	1.8×10^3
5	$AnN_2\cdot$	$\rightarrow$	$An\cdot + N_2$	k_5	1.0×10^6
6	$An\cdot + MeCN$	$\rightarrow$	AnH*(1)* $+ NCCH_2\cdot$	k_6	5.0×10^4
7	$An\cdot + AnN_2^+$	$\rightleftharpoons$	$AnN{=}NAn^{+\bullet}$	k_7	3.0×10^7
				k_{-7}	1.0
8	$AnN{=}NAn^{+\bullet} + Cu^+$	$\rightarrow$	$AnN{=}NAn$*(1)* $+ Cu^{2+}$	k_8	3.5×10^3
9	$An\cdot + Cu^+$	$\rightleftharpoons$	$(Cu^{II}An)^+$	k_9	7.5×10^8
				k_{-9}	5.0
10	$NCCH_2\cdot + Cu^+$	$\rightarrow$	$(Cu^{II}CH_2CN)^+$	k_{10}	5.0×10^8
11	$(Cu^{II}An)^+ + Cu^+$	$\rightarrow$	$(Cu^{I}An) + Cu^{2+}$	k_{11}	2.0×10^1
12	$(Cu^{I}An) + AnN_2^+$	$\rightarrow$	$AnN{=}NAn$*(2)* $+ Cu^+$	k_{12}	1.0×10^5
13	$(Cu^{II}An)^+ + (Cu^{II}An)^+$	$\rightarrow$	$(Cu^{III}An_2)^+ + Cu^+$	k_{13}	5.0×10^3
14	$(Cu^{III}An_2)^+$	$\rightarrow$	$4,4'\text{-}An_2 + Cu^+$	k_{14}	6.0×10^2
15	$(Cu^{III}An_2)^+ + H_2O$	$\rightarrow$	$AnOH$*(1)* $+ AnH$*(2a)* $+ Cu^+$	k_{15}	5.0×10^1
16	$(Cu^{II}An)^+ + (Cu^{II}CH_2CN)^+$	$\rightarrow$	$\{Cu^{III}An(CH_2CN)\}^+ + Cu^+$	k_{16}	5.0×10^3
17	$\{Cu^{III}An(CH_2CN)\}^+$	$\rightarrow$	$AnCH_2CN + Cu^+$	k_{17}	1.0×10^3
18	$\{Cu^{III}An(CH_2CN)\}^+ + H_2O$	$\rightarrow$	AnH*(2b)* $+ NCCH_2OH + Cu^+$	k_{18}	2.5×10^1
19	$\{Cu^{III}An(CH_2CN)\}^+ + H_2O$	$\rightarrow$	$AnOH$*(2)* $+ MeCN + Cu^+$	k_{19}	2.5×10^1
20	$(Cu^{II}An)^+ + H_2O$	$\rightarrow$	AnH*(2c)* $+ OH^- + Cu^{2+}$	k_{20}	1.0×10^{-4}
21	$(Cu^{II}CH_2CN)^+ + H_2O$	$\rightarrow$	$MeCN + OH^- + Cu^{2+}$	k_{21}	6.0×10^{-3}
22	$Cu^{2+} + HPO_4^{2-}$	$\rightleftharpoons$	$CuHPO_4$	k_{22}	2.0×10^7
				k_{-22}	1.0×10^4

[a] An ≡ 4-methoxyphenyl; Cu^+ ≡ a cation $[Cu^I(NCMe)_n(OH_2)_{(4-n)}]^+$, ($n = 1 - 3$), derived from **2**; solvent-derived ligands are not indicated for organocopper complexes.
[b] Units as appropriate to the molecularity of reaction.
[c] A^-, see Scheme 2 for structure; when reaction 22 is included, it is immaterial whether the inorganic product is expressed as $Cu^{2+} + HPO_4^{2-}$ or $CuHPO_4$.

Scheme 5

Reactions 11–21 are those proposed for organocopper intermediates; where water is a reactant (in the sense of supplying OH^- to carbon in hydrolysis or H^+ in protonolysis), its concentration in the mixed solvent (27.7 mol dm^{-3}) was used (as for MeCN mentioned previously) and the ascribed constants are therefore of second order. The organocopper-mediated route to AnN=NAn (*i.e.* **5**) is represented by reactions 11 and 12. The value assigned to k_{11}, found by trial and error, is crucial since it, together with k_7, determines the distribution of the major product. AnN=NAn derived by the organocopper route is labelled (*2*). The value given to k_{12} is sufficiently high to ensure that residual ($Cu^{I}An$) is negligible at the end of the simulation.

Some of the remaining reactions are grouped to simplify the allocation of rate constants. Reactions 13 and 16 which both give rise to Cu(III) intermediates are assigned rate constants of the same value. The phenol-yielding hydrolyses, reactions 15 and 19, are given rate constants differing by a factor of two as reaction 15 has a statistical advantage of this magnitude. Reaction 18 is allocated the same rate constant as reaction 19 as they are alternative hydrolyses of $\{Cu^{III}An(CH_2CN)\}^+$ and there is no basis on which to discriminate between them; furthermore, it also ensures that the model gives **6** and organocopper(III)-derived **3** in equal amounts. Reaction 18 generates an end-product, methanal cyanhydrin, which is not actually observed; it, or its dissociation products, CH_2=O and HCN, would be expected to be retained in the aqueous phase in pre-analysis work-up. Reaction 20 formally allows protonolysis of $(Cu^{II}An)^+$ but the constant assigned ensures the reaction is of negligible importance, producing $<0.2\%_N$ of products. There would be leeway within the model to increase k_{20} by decreasing or eliminating k_{18}; reactions 18 and 20 both give protonolysis-derived **3** in amounts which are minor in comparison to that from reaction 15 [see ESI, Tables S4(i)–S4(iii)‡].

The model was developed in two stages: first, without reaction 22 which represents the withdrawal of the catalytic HPO_4^{2-} by formation of a salt with the Cu^{2+} produced in the overall reaction; in the second stage, reaction 22 was included but without alteration of the first-stage rate constants. The magnitudes of the rate constants assigned to reaction 22 are arbitrary but their relative sizes are based on a published equilibrium constant for aqueous conditions:

$$Cu^{2+} + HPO_4^{2-} \rightleftharpoons CuHPO_4 \log K = 3.27 \text{ at } 25\ ^\circ C,\ I_{aq} = 0.1.^{58}$$

Only the equilibrium pairing of the two ions is considered, no attempt being made to model crystal nucleation and precipitation proper though, in reality, the latter must reduce the availability of $CuHPO_4$ for the reverse of reaction 22. Reaction 22 is the only reaction in Scheme 5 according a reactant role to Cu^{2+}.

The Scheme is necessarily an oversimplification, for example in omitting the species T of Scheme 2 as previously mentioned and not addressing *how* the ligand transfers of reactions 13 and 16 occur. Presumably, they could occur *via* transient binuclear complexes with bridging An (or An and $NCCH_2$) groups. Indeed, the reductive elimination of **4** and **7** could conceivably occur directly from such complexes in a manner similar to the case of cyanogen[44] but mononuclear copper(III) complexes bearing two carbon-bound ligands are necessary for our proposed concerted formation of **6** and **3** (*cf.* Scheme 4).

The decision to exclude AnCN (*i.e.* **8**) from the simulation was made on the following grounds. Ingold and co-workers[59] had reported a rate constant of 4×10^3 s^{-1} at 298 K for the irreversible cyclisation of $N{\equiv}C(CH_2)_3CH_2^{\bullet}$ to $(CH_2)_4C{=}N^{\bullet}$. The effective rate under typical conditions for addition of $An^{\bullet}$ to MeCN would be expected to be smaller on account of the loss of translational entropy in this bimolecular reaction; furthermore, the yield of **8** from fragmentation of the adduct would be reduced if the initial addition were reversible. Preliminary modelling with no reversibility ($An^{\bullet}$ + MeCN → **8** + $Me^{\bullet}$) using a rate constant of 1×10^3 dm^3 mol^{-1} s^{-1} gave normalised yields of **8** $< 1\%_N$ in the conditions of subset (a) of Table 8.

We considered Cohen's proposal[5] for the formation of $(Cu^{III}Ar_2)^+$ [see (iii) above] and adopted similar reactions for the formation of $(Cu^{III}An_2)^+$ and $\{Cu^{III}An(CH_2CN)\}^+$ as alternatives to reactions 13 and 16:

$$An^{\bullet} + (Cu^{II}An)^+ \rightarrow (Cu^{III}An_2)^+$$

$$An^{\bullet} + (Cu^{II}CH_2CN)^+ \rightarrow \{Cu^{III}An(CH_2CN)\}^+$$

and

$$NCCH_2^{\bullet} + (Cu^{II}Ar)^+ \rightarrow \{Cu^{III}An(CH_2CN)\}^+$$

However, in order to match the experimental yields of **4**, **6** and **7** in the context of the precedented reactions used in Scheme 5, it was necessary to assign rate constants of at least 2×10^9 dm^3 mol^{-1} s^{-1} to each of these processes which had detrimental effects on the distributions of other products; we ultimately abandoned this approach.

Simulated product distributions. Fig. 3 compares the simulated and experimental distributions of products in subset (a) of Table 8 (see ESI, Table S4(i) for the calculated values‡). In Fig 3a, comparing first the simulated normalised percentage yields with and without inclusion of reaction 22 in Scheme 5, it is clear that for values of $([\mathbf{2}]/[\mathbf{1}])_{init} > \sim 1$, similar behaviour is obtained

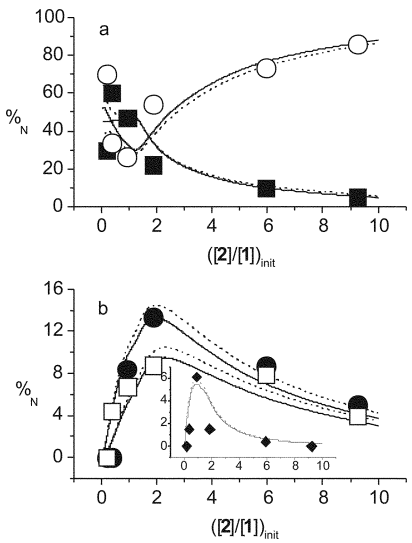

Fig. 3 **a** Variation in normalised percentage yields of **5** (open circles) and **3** (filled squares) as functions of $([\mathbf{2}]/[\mathbf{1}])_{init}$. **b** Variation in normalised percentage yields of **4** (open squares) and **6** (filled circles) with **7** (inset) as functions of $([\mathbf{2}]/[\mathbf{1}])_{init}$. Individual points are the experimental values of subset (a) of Table 8; dashed curves: values calculated *via* Scheme 5 without reaction 22; continuous curves: values calculated *via* Scheme 5 including reaction 22.

irrespective of whether or not reaction 22 is included in the model: when reaction 22 *is* included, simulated yields are, at the most, 3%$_N$ larger for **5** and 1.5%$_N$ smaller for **3** than are the cases if reaction 22 is excluded. For $([\mathbf{2}]/[\mathbf{1}])_{init} < 1$, however, different behaviour is observed: simulated yields of **3** decrease when reaction 22 is included but increase if it is excluded and simulated yields of **5** peak at ~50%$_N$ when reaction 22 is included but at ~40%$_N$ when it is excluded. The consequence of these differences is that the curves representing the trends in simulated yields of **3** and **5** intersect twice when the model includes reaction 22 but only once when it is not included.

The distribution of the six sets of experimental data in Fig. 3a is reasonably well described by the continuous simulation curves corresponding to the model which includes reaction 22. It is noticeable that when experimental points occur at abscissa values close to those of the intersections of the simulated curves, the paired experimental points for **3** and **5** do not coincide but are displaced equally (~15%$_N$) in opposite directions from their respective simulations. We suggest the reason for this stems from the reciprocal relationship between the yields of the two products and the fact that the normalised percentage yield of any individual product accumulates error from the measurements of all other products [see eqn. (5)]. Fig. 3b shows that the Scheme 5 model with inclusion of reaction 22 simulates the distributions of products **4**, **6** and **7** satisfactorily reproducing their maxima at the appropriate values of $([\mathbf{2}]/[\mathbf{1}])_{init}$.

Fig. 4 compares the simulated and experimental distributions of products in subset (b) of Table 8 [see ESI, Table S4(ii) for calculated values‡]. In Fig 4a and b for high values of $([\mathbf{2}]/[\mathbf{1}])_{init}$, again there is little difference between simulated yields whether or not reaction 22 is included and the simulated yields are close to the experimental values. However, for $([\mathbf{2}]/[\mathbf{1}])_{init} < 3$, the simulated yields of **5** determined by the inclusion or otherwise of reaction

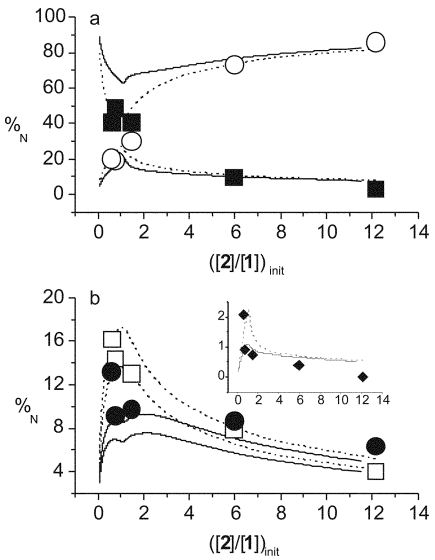

Fig. 4 **a** Variation in normalised percentage yields of **5** (open circles) and **3** (filled squares) as functions of $([\mathbf{2}]/[\mathbf{1}])_{init}$. **b** Variation in normalised percentage yields of **4** (open squares) and **6** (filled circles) with **7** (inset) as functions of $([\mathbf{2}]/[\mathbf{1}])_{init}$. Individual points are the experimental values of subset (b) of Table 8; dashed curves: values calculated *via* Scheme 5 without reaction 22; continuous curves: values calculated *via* Scheme 5 including reaction 22.

22 differ by 10–20%$_N$. Furthermore, the experimental yields of **5** are much lower than either of the simulations especially those which arise from inclusion of reaction 22. Unsurprisingly, given the interdependence of normalised yields, the experimental yields of the other products are also poorly modelled. Product distributions in subset (c) of Table 8, where $([\mathbf{2}]/[\mathbf{1}])_{init} < 1$ are also poorly modelled [see ESI, Table S4(iii)].

We suggest that these shortcomings of the simulation occur because additional reactions intervene in the relatively concentrated solution conditions of subsets (b) and (c) giving products which are not included in the model or not observed experimentally. When $[\mathbf{1}] \gg [\mathbf{2}]$, much of **2** is consumed in the reduction step (reaction 4) and relatively less remains for intercepting An$^\bullet$ in reaction 9. As a consequence, other reactions of An$^\bullet$ become apparent: additions to the aromatic ring of **1** hence giving the asymmetrical biaryls **9** and **10** (*cf.* Scheme 3), and addition to MeCN giving AnCN, **8**, after elimination of Me$^\bullet$. However, the shortfall in the experimental yields of the azoarene, **5**, compared to the calculated expectation, is too great to be accounted for by these diversions of An$^\bullet$ to the above-mentioned secondary products alone. If most **2** is consumed by the reduction step, then An$^\bullet$ will certainly add to the azo-function of **1** to give AnN=NAr$^{+\bullet}$ but there may then not be sufficient **2** to reduce all of the latter. If, additionally, this cation radical should have significant persistence, it would be expected to be an efficient trap (particularly if it is a π-radical) for other more transient radicals in the system such as AnN$_2^\bullet$ and An$^\bullet$; it might also oxidise **6** (AnOH) to give AnO$^\bullet$, which could also be trapped. The failure to observe yields of **6** in entries 11–13 of Table 8 could stem from such a reaction between AnN=NAr$^{+\bullet}$ and **6**; we have previously proposed this reaction in another context.[60] We envisage that radical trapping by AnN=NAr$^{+\bullet}$ could initiate formation of the well-known diazo-tar which forms on manipulation of diazonium salts in weakly alkaline conditions.[61]

The modelling by Scheme 5 provides support for a role for the cation radical AnN=NAr$^{+\bullet}$. For example, for $[\mathbf{1}] = 0.08$ mol dm^{-3} and [**2**] in the range 0.001–0.01 mol dm^{-3}, conditions which include those of entries 11–13 of Table 8, calculated yields of the cation radical result which range from 0.56 to 0%$_N$ when reaction 22 is excluded but from 19.14 to 1.07%$_N$ when it is included [see ESI, Table S4(iii)‡]. The value of k_8 was chosen to ensure that the negligible cation radical was calculated to remain at the end of the run in the conditions of subsets (a) and (b). If, in reality, $k_8 < 3.5 \times 10^3$ dm^3 mol^{-1} s^{-1}, AnN=NAr$^{+\bullet}$ might be formed in concentrations which enable it to trap other radicals in amounts sufficient to reduce the experimental yield of **5**. Independent evidence of persistent azobenzene cation radicals in fluid solution is equivocal.[62]

The strongest evidence for the formation of unobserved products (*i.e.* diazo-tar which does not undergo GC) comes from the low experimental accountabilities of **1** in observed products (Table 8) and their comparison with calculated accountabilities [see ESI, Tables S4(i)–S4(iii)‡]. Fig. 5a shows a graphical comparison of the experimental accountabilities (all subsets) with values calculated *via* Scheme 5 (with inclusion of reaction 22) as a function of $([\mathbf{2}]/[\mathbf{1}])_{init}$ (plotted logarithmically to disperse the low values). The values calculated for the conditions of subsets (b) and (c) lie on a common curve whereas those calculated for subset (a) fall somewhat lower. If the stoichiometry of the overall process is taken as the value of $([\mathbf{2}]/[\mathbf{1}])_{init}$ at which the calculated

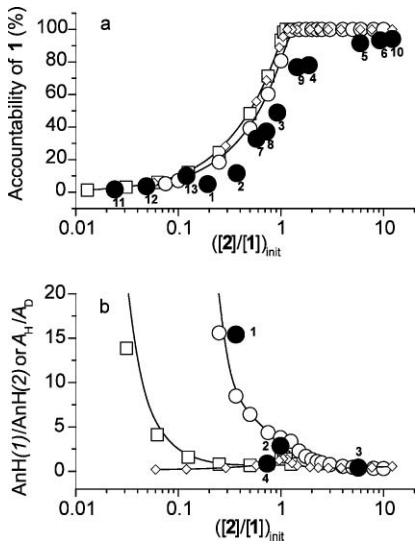

Fig. 5 **a** Comparison of calculated with experimental accountabilities (%) of **1** as functions of $([\mathbf{2}]/[\mathbf{1}])_{init}$. Open circles: calculations for subset (a); small diamonds: calculations for subset (b); open squares: calculations for subset (c); filled circles: experimental values (all subsets), labelled with the entry number of Table 8. **b** Comparison of calculated with experimental ratios of H-abstraction- and protonolysis-derived AnH (**3**) as functions of $([\mathbf{2}]/[\mathbf{1}])_{init}$. Open circles: calculations for subset (a); open diamonds: calculations for subset (b); open squares calculations for subset (c); filled circles experimental A_H/A_D values labelled with the entry number of Table 9.

accountability of **1** becomes 100%, that of subset (a) is 1.25 whereas that of the more concentrated conditions of subsets (b) and (c) is 1.15. Although the experimental accountabilities approach the calculated values for high and low values of $([\mathbf{2}]/[\mathbf{1}])_{init}$, at intermediate values between 0.2 and 3, the experimental values fall short of the appropriate calculated values by 15–25%. If, under these conditions, reactions of a precursor (*i.e.* AnN=NAr$^{+\bullet}$) to one observed product (*i.e.* **5**) divert radicals that give rise to all the observed products to material that is not observed (*i.e.* diazo-tar), the shortfalls in the experimental accountability of **1** and in the normalised yield of **5** and hence, the perturbed normalised yields of the remaining products, is understandable.

In Fig. 5b are plotted, *versus* $([\mathbf{2}]/[\mathbf{1}])_{init}$, AnH(*1*)/AnH(*2*) normalised percentage ratios calculated *via* the model of Scheme 5 with inclusion of reaction 22. The calculations are part of those carried out for the three solution compositions of the subsets of Table 8 [see ESI, Tables S4(i)–S4(iii)‡]. These ratios therefore simulate the relative proportions of **3** derived by H-abstraction from MeCN and by protonolysis of organocopper intermediates. For comparison, also plotted in Fig. 5b are the experimental isotopic mass spectral peak area ratios, A_H/A_D, labelled by their entry numbers in Table 9. The reasonable agreement of the experimental and predicted ratios indicates that the model gives a satisfactory account of the separate contributions of the H-abstraction and protonolysis pathways to the single product **3** (AnH). The least satisfactory agreement is found for point 1 where the experimental ratio is larger than that predicted by a factor of 1.8. However, as a function of $([\mathbf{2}]/[\mathbf{1}])_{init}$, AnH(*1*)/AnH(*2*) changes sharply in the region of point 1 and better agreement might have been obtained by assigning a somewhat larger value to k_6; also, the larger than predicted value for A_H/A_D could, in part, be experimental artefact: *protic* buffer salt was used in the deuteriated solvent which would lead to some dilution of the heavier isotope. The general agreement of experiment and model lends credence to the assumption in Scheme 5 that protonolysis is coupled with the hydrolysis of Cu(III) intermediates which gives rise to the phenol **6** (*cf.* reactions 15, 18 and 19).

Nitrogen evolution. The model of Scheme 5, with inclusion of reaction 22, was used to calculate the yields of N_2 as functions of time for two solutions, the one with the initial concentrations [**1**] and [**2**] each 0.01 mol dm^{-3} and buffer salt $B_{50} = 0.081$ mol dm^{-3}, the other with initial concentrations [**1**] = 0.01 mol dm^{-3} and [**2**] = 0.02 mol dm^{-3} and buffer salt $B_{50} = 0.025$ mol dm^{-3}. The yields of N_2 were expressed as the percentage of that theoretically available in **1** though both the calculated percentages, Q_{calc}, and experimental percentages, Q_{exp}, are expected to be significantly less than this amount since nitrogen is retained in the azoarene co-product **5**. In Fig. 6 the continuous curve 1 shows the variation with time of the percentage, $Q_{calc(H)}$, calculated for the higher concentration of buffer salt, and the associated discrete points the variation of the corresponding experimental values $Q_{exp(H)}$; the continuous curve 2 shows the variation with time of the percentage, $Q_{calc(L)}$, calculated for the lower concentration of buffer salt and the discrete points the corresponding experimental values, $Q_{exp(L)}$. [For Q_{exp} data see ESI, Table S2(i), columns Q_2(A) and Q_1(C); for Q_{calc} data see Table S5.‡]

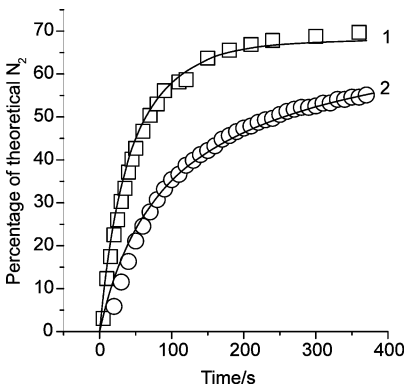

Fig. 6 Comparison of calculated with experimental rates of N_2 evolution. Curve 1: calculated values for [**1**] = [**2**] = 0.01 mol dm^{-3} and B_{50} = 0.081 mol dm^{-3}, squares: corresponding experimental values; curve 2: calculated values for [**1**] = 0.01 mol dm^{-3}, [**2**] = 0.02 mol dm^{-3} and B_{50} = 0.025 mol dm^{-3}, circles: corresponding experimental values.

The model clearly satisfactorily reflects the N_2 evolution behaviour of the system, to be expected perhaps given that the overall rate determining rate constant (k_3) was inferred from the gasometric experiments of which that giving $Q_{exp(L)}$ was a part and both curves correspond to conditions within subset (a) of Table 8 which were assumed in allocating rate constants to the other reactions of the scheme.

Adaptation for electron-withdrawing substitution. It has already been noted (Introduction) that, on reduction of substituted diazonium ions by Cu(I), the relative yield of symmetrically substituted azoarene and biaryl varies with the electronic nature of the substituent[2,5] and the reaction has been developed as a

synthetic route to biaryls.[63] For the highest values of $([\mathbf{2}]/[\mathbf{1}])_{init}$ examined in subsets (a) and (b) (Table 8, entries 6 and 10), the experimental azoarene/biaryl ratio is 21 and the model represented by Scheme 5 (including reaction 22) gives simulated values in excellent agreement [see ESI, Tables S4(i) and S4(ii)‡]. As expected for the strongly electron-donating 4-OMe substituent, the ratio $\gg 1$. It was of interest to see how adjustments to rate constants in Scheme 5, made to represent a change of substituent character to electron-withdrawing, would impact on the predictions of the model, in particular on the azoarene–biaryl ratio. Although we have not attempted to simulate the behaviour of a real example with an electron-withdrawing substituent, reasonable adjustments to the rate constants allow the azoarene–biaryl ratio to be inverted showing that the Scheme is compatible with known chemical behaviour. Details are given in the ESI, Table S6.‡

Conclusions

$[Cu^{I}(NCMe)_4]^+$ in MeCN and the cations $[Cu^{I}(NCMe)_n(OH_2)_{(4-n)}]^+$, ($n$, 1–3), derived from it in aqueous MeCN, fail to reduce 4-methoxybenzenediazonium ion at an appreciable rate but the reaction is catalysed in the presence of phosphate buffer. Investigation of the reaction mechanism indicates the catalytic species to be HPO_4^{2-} which associates reversibly with the diazonium ion in the overall rate-determining step to give an adduct that, in turn, undergoes reduction by one or more of cations $[Cu^{I}(NCMe)_n(OH_2)_{(4-n)}]^+$, ($n$, 1–3). The nature of the catalysis thus appears to be the bridging of the reactant cations by the di-anionic catalyst, a process which overcomes coulombic repulsions and assists in the geometry changes needed for electron transfer to occur. The reaction is auto-inhibitory in the sense that Cu^{2+} produced by the reduction precipitates HPO_4^{2-} and thereby depletes the available catalyst.

4-Methoxyphenyldiazenyl radical, the presumed initial reduction product, undergoes rapid loss of N_2 to form 4-methoxyphenyl radical, An$^{\bullet}$. As primary reactions, this radical abstracts hydrogen from MeCN, and adds to the reactant diazonium ion and to Cu(I) species giving, respectively, the cation radical of 4,4′-dimethoxyazobenzene and the adduct $(Cu^{II}An)^+$. The ramifications of these various primary reactions produce nine compounds which are recognised and quantified by GC; pathways leading to these products are suggested. 4-Methoxyphenol is a product unexpected in the reducing medium. It is suggested to arise *via* hydrolysis of $(Cu^{III}An_2)^+$ formed by disproportionation of $(Cu^{II}An)^+$. Although disproportionation has not been reported for comparable aliphatic Cu(II) complexes, it seems plausible given that these are odd-electron species. A further tentative suggestion is that, concerted with the hydrolysis of the Cu^{III}–An bond, protonolysis of the developing Cu^{I}–An bond also occurs, thus generating 4-methoxyphenol and organocopper-derived methoxybenzene in equal amounts; the formation of 4,4′-dimethoxybiphenyl is suggested to occur by reductive elimination from $(Cu^{III}An_2)^+$. 4,4′-Dimethoxyazobenzene is suggested to arise *via* two reactions: reduction of its cation radical mentioned above and addition of $(Cu^{I}An)$, produced by reduction of $(Cu^{II}An)^+$, to the initial diazonium ion.

A computer model of the proposed reaction scheme succeeds in simulating the observed trends in the proportions of the five principal products as functions of the relative concentrations of reactants in conditions where reactants are relatively dilute and/or where Cu(I) is in excess over the diazonium ion. It also gives a satisfactory account of the distribution of hydrogen isotopes in methoxybenzene produced by different pathways involving H-abstraction from MeCN or deuteronolysis of organocopper intermediates and of the evolution of N_2 as a function of time. For more concentrated conditions, where the diazonium ion is in excess, the scheme is less successful in simulating the experimental product distribution owing to the probable intervention of reactions leading to polymeric material (diazo-tar) which is not analysable by GC but the formation of which is indicated by the reduced accountability of initial diazonium ion as observed products. The rate constants assigned to the steps of the scheme cannot all be 'chemically correct' as several are arbitrary and a somewhat different set of arbitrary assignments could probably give a comparable account of the product distribution but it is suggested that the reactions proposed provide a basis for understanding the chemistry observed and the assigned constants reflect their relative significance. Rational changes to some of the rate constants allow the scheme to model the dependence of the azoarene–biaryl ratio on substituent character.

Experimental

(i) Starting materials

4-Methoxybenzenediazonium tetrafluoroborate, 1. The required diazonium salt was prepared and characterised as previously described.[7]

Tetrakis(acetonitrile)copper(I) tetrafluoroborate, 2. The tetrafluoroborate salt of the reductant was made by adaptation of the method of Kubas for the hexafluorophosphate,[15] using 50% HBF_4 in place of 60–65% HPF_6. It did not melt simply: thermal analysis showed decomposition to commence at 130 °C and involve two endotherms, the first corresponding to a loss of 26.3% of initial mass (2 × MeCN) at 157 °C and the second to a loss of 47.5% of initial mass (BF_3 + 2 × MeCN) at 255 °C; ν_{max}(Nujol)/cm^{-1} 2304 and 2276 (C≡N), 1029 (BF_4^-), lit.[15] 2305, 2277 cm^{-1}.

Acetonitrile. Solvent of HPLC grade (Fisher) was used as received.

Reaction media. Detail of the preparation and characterisation of the various aqueous acetonitrile buffer solutions used as reaction media is given in ESI.‡

(ii) Spectrophotometric rate measurements at variable phosphate buffer concentration

4-Methoxybenzenediazonium tetrafluoroborate, **1** (22.2 mg, 0.1 mmol) was dissolved in the required aqueous acetonitrile buffer in a 100 cm^3 volumetric flask to give a master solution of concentration 1×10^{-3} mol dm^{-3}. An aliquot of this solution (7.5 cm^3) was further diluted to 100 cm^3 with the same solvent to give a working solution of 7.5×10^{-5} mol dm^{-3} which was thermally equilibrated at 298 K. An aliquot (3.0 cm^3) of the working solution was placed in a thermostated cuvette of path-length 1 cm in the spectrophotometer (Cintra 5) with the same acetonitrile–buffer mixture in a similar cuvette in the compensating beam. Solutions of tetrakis(acetonitrile)copper(I)

tetrafluoroborate, **2**, in MeCN (0.2 mol dm^{-3}) were added to the sample cuvette by micropipette such that [**2**]/[**1**]$_{init}$ fell in the range 5–40 as convenient and the decay in absorption of the diazonium ion at λ_{max} 312 nm was monitored at 298 K (see ESI, Fig. S1‡). Runs were duplicated for each aqueous acetonitrile buffer and at least three measurements were made of each pseudo-first order rate constant k_{obs} found from a particular diazonium solution. Each rate constant k_{obs} is thus normally the mean of six determinations (see Table 2).

(iii) Spectrophotometric rate measurements at constant pH and variable ionic strength in 50% aqueous acetonitrile buffer

Into each of seven 25 cm^3 volumetric flasks (*a–g*) were dispensed 12.5 cm^3 of a solution of **1** (3×10^{-4} mol dm^{-3}) in aqueous buffer of pH 7 and $B_{aq} = 0.15$ mol dm^{-3}. To each flask was then added an individual volume (0, 2, 4,$\cdots$12 cm^3) of an aqueous solution of KNO_3 (0.25 mol dm^{-3}) and the flasks were made up to the mark with deionised water. Each completed flask thus contained **1** at a concentration of 1.5×10^{-4} mol dm^{-3} in aqueous buffer (pH$_{aq}$ 7 and $B_{aq} = 0.075$ mol dm^{-3}) and a particular concentration of KNO_3 (0, 0.02, 0.04,$\cdots$0.12 mol dm^{-3}).

Into each of seven further 25 cm^3 volumetric flasks (*A–G*) were dispensed 12.5 cm^3 of MeCN and then, with thermal equilibration to compensate for endothermic mixing, each was made up to the mark with the correspondingly lettered buffer solution from flasks *a–g.* The final working solutions *Aa–Gg* thus contained **1** at a concentration of 7.5×10^{-5} mol dm^{-3} in 50% v/v aqueous MeCN buffer, $B_{50} = 0.0375$ mol dm^{-3} and individual concentrations of KNO_3 (the pH$_{50}$ varied slightly with the ionic strength about a mean value of pH$_{50}$ = 7.85, see Table 4). They were thermally equilibrated at 298 K.

To aliquots (3 cm^3) of these solutions in cuvettes of 1 cm path-length thermostated at 298 K were added by micropipette, 0.0225 cm^3 of **2** in MeCN (0.20 mol dm^{-3}) and the decay of the absorbance of the diazonium ion at 312 nm monitored spectrophotometrically with a similar cuvette containing 50% v/v aqueous MeCN buffer ($B_{50} = 0.0375$ mol dm^{-3}) in the compensating beam. The final absorbance in these runs increased slightly with increasing concentration of KNO_3 which has a small absorbance at 312 nm. The pseudo-first order rate constants obtained are given in Table 4.

(iv) Spectrophotometric rate measurements at variable pH and constant ionic strength in 50% aqueous acetonitrile buffers

Buffer ratios, $r_B = [H_2PO_4^-]/[HPO_4^{2-}]$, corresponding to pH$_{aq}$ values 6.00, 6.25, 6.50, 6.75, 7.00, 7.25 and 7.50 were calculated for aqueous buffers *via* the Henderson–Hasselbalch equation and the pK_a (6.75) of KH_2PO_4 at 298 K and ionic strength 0.1 mol dm^{-3}.[58] From these ratios, the requirements of [KH_2PO_4] for a fixed value of [K_2HPO_4] of 0.02 mol dm^{-3} were determined for each pH. A series of buffers of ionic strength 0.2 mol dm^{-3} was then made up by addition of appropriate volumes of solutions of KH_2PO_4 and KNO_3 (each 0.3 mol dm^{-3}) to a solution of $K_2HPO_4 \cdot 3H_2O$ (40 cm^3, 0.05 mol dm^{-3}) and dilution to 100 cm^3 in standard flasks.

Working solutions were made up by dilution of 25 cm^3 of a solution of **1** in MeCN (1.5×10^{-4} mol dm^{-3}) to 50 cm^3 with each of these buffers (again with allowance for recovery from the endotherm). Reaction was initiated by addition of a solution of **2** in MeCN (0.0225 cm^3, 0.2 mol dm^{-3}) by micropipette to a 3 cm^3 aliquot of working solution in a cuvette of path-length 1 cm. Again the decay of absorbance of **1** at 312 nm was monitored at 298 K under pseudo-first order conditions (see Table 5).

Analogous rate measurements were also made in which the 'buffers' comprised five aqueous solutions of KH_2PO_4 in the concentration range 0.1–0.2 mol dm^{-3} and at ionic strength 0.2 mol dm^{-3} (adjustment with KNO_3). The pH$_{50}$ values for the derived mixed solutions were essentially constant at 5.57 ± 0.01.

(v) Measurement of the rates of nitrogen evolution

The displacement cell used for the measurement of the N_2 evolved from decompositions of diazonium ions has been described previously.[23] In the present experiments, a three-necked 250 cm^3 round bottom flask was immersed in a water bath thermostated at 298 K and fitted with an efficient gas-tight overhead stirrer, a small pressure-equalising tap-funnel and a gas-outlet tube leading to the displacement cell. 4-Methoxybenzenediazonium tetrafluoroborate, **1**, (0.222 g, 1 mmol), accurately weighed, was added to the flask with 50 cm^3 buffer (pH$_{aq}$ 7, $B_{aq} = 0.05$ mol dm^{-3}) and (50 − *x*) cm^3 of MeCN where *x* cm^3 is the volume of the solution of **2** (0.2 mol dm^{-3}) to be added *via* the tap-funnel. The solution was stirred to ensure dissolution of **1** and recovery from the endotherm. The addition of the solution of **2** was then made as rapidly as practicable with efficient stirring. After the latter addition, the total volume of solution was 100 cm^3, the composition of the solvent was 50% v/v aqueous MeCN buffer (pH$_{50}$ 8, $B_{50} = 0.025$ mol dm^{-3}), the initial concentration of **1** was 0.01 mol dm^{-3} and that of **2** was 0.02, 0.01 or 0.005 mol dm^{-3} according as *x* was 10, 5 or 2.5 cm^3; an additional measurement was made in which the aqueous buffer was prepared as [KH_2PO_4] = 0.1 mol dm^{-3}, [K_2HPO_4] = 0.062 mol dm^{-3} whence B_{aq} = 0.162 mol dm^{-3}and $B_{50} = 0.081$ mol dm^{-3}. The N_2-evolution data are tabulated in the ESI, Table S2(i).‡

(vi) Measurements of the product distribution

An aqueous phosphate buffer (pH$_{aq}$ 7) was prepared containing KH_2PO_4 and K_2HPO_4 at respective concentrations of 0.100 and 0.062 mol dm^{-1} and mixed in equal volumes with MeCN to give an aqueous MeCN buffer, pH 7.9, $B_{50} = 0.081$ mol dm^{-3}. A chosen weight of **1** was dissolved in the aqueous MeCN buffer (*x* cm^3) plus additional aqueous buffer (*y* cm^3) and a solution of **2** in MeCN (0.1923 mol dm^{-3}, *y* cm^3) was added. The volumes *x* and *y* were chosen so that (*x* + 2*y*) = 50 cm^3 and *y* cm^3 of the solution of **2** contained the requisite amount of **2**. The mixture was stirred for 2 h at 298 K and then added to an aqueous solution of di-sodium 2-naphthol-3,6-disulfonate (0.17 mol dm^{-3}, 50 cm^3) in order to sequester any unreacted **1**. A solution of the internal standard for GC analysis, dibenzofuran in diethyl ether (0.0100 mol dm^{-3}, 10 cm^3), was added and the mixture was extracted with more ether. The ether extracts were reduced in volume at ambient temperature before GC analysis. This was performed using an SE-54 column (30 m, 5% phenyl) in a Varian 3350 chromatograph served by a Varian Star workstation with the temperature programme: 60 °C for 5 min, then 16 °C per min to 290 °C and held for 5 min.

(vii) Measurements of hydrogen isotopic ratios in methoxybenzene

Typically a buffer solution ($B_{aq} = 0.16$ mol dm^{-3}) was prepared by dissolving KH_2PO_4 (0.1998 g) and K_2HPO_4 (0.1602 g) in 15 cm^3 D_2O. In 5 cm^3 aliquots of such a solution was dissolved the required amount of **1** and $(5 - x)$ cm^3 MeCN were added where x cm^3 is the volume of a MeCN solution of **2** (0.1923 mol dm^{-3}) needed to give the required concentration of **2**. After stirring for 2 h, the solutions were worked up as in (vi) above and analysed by GC-MS [Fisons Analytical (VG) Autospectrometer directly coupled to a gas chromatograph]. The integrated areas of the peaks at m/z 108 and 109 in the mass spectrum of **3**, A_H and A_D, respectively (corresponding to AnH and AnD) were measured and the latter was adjusted for the natural abundances of ^{13}C, ^{17}O and ^2H in **3**. Thus, taking 1.11, 0.04 and 0.016%,[64] respectively, as the natural abundances of ^{13}C, ^{17}O and ^2H, a correction of $(7 \times 0.0111 + 0.0004 + 8 \times 0.00016)A_H = 0.0794A_H$ was subtracted from A_D. The corrected isotopic ratios calculated for **3** thus are $A_H/(A_D - 0.0794\ A_H)$; these are given in Table 9.

Authentication of reaction products. Organic reaction products were authenticated by comparison of their mass spectra and GC retention times with those of commercial materials except for 4,4′-dimethoxyazobenzene, **5** and 2,4′- and 3,4′-dimethoxy-biphenyls, **9** and **10**.

4,4′-Dimethoxyazobenzene, 5. 4-Methoxyaniline (2 g) was diazotised by dissolution in hydrochloric acid [concentrated hydrochloric acid (2.5 cm^3) plus water (6 cm^3)], chilling to 0–5 °C, and addition of $NaNO_2$ (1.5 g). After stirring for 30 min, excess of $NaNO_2$ was destroyed by addition of urea and the solution, still chilled, was added to an aqueous solution of phenol (1.5 g) and sodium hydroxide (1 g). After stirring for 10 min, this mixture was acidified and extracted with ether. The ether was then removed and the crude 4-hydroxy-4′-methoxyazobenzene (1.8 g) was dissolved in MeOH (40 cm^3); Na metal (0.3 g) was added and the solution stirred under N_2. Once the Na had dissolved, MeI (5 g) was added and the mixture heated under gentle reflux overnight. The solution was diluted with water (250 cm^3) and the product extracted into ether. The extract was washed with NaOH solution (pH 13–14) and with water. After drying, removal of the solvent gave 4,4′-dimethoxyazobenzene, **5**, (2 g, 53%), mp 160–161 °C, lit.[65a] 166.5–167 °C; m/z 242 (53%, M$^+$), 135 (22), 107 (100), 92 (44), 77 (48) and 64 (23); ν_{max}(Nujol)/cm^{-1} 1594 (N=N), 1250 (C–O–C), 1021 (C–O–C); δ_H (270 MHz, $CDCl_3$) 3.87 (s, 6H), 7.00 (d, J 9.0, 4H), 7.88 (d, J 9.0, 4H); δ_C(67.9 MHz, $CDCl_3$) 55.5, 114.1 (2C), 124.3 (2C), 147, 161.5; lit.[65b] for comparable characterisation spectra.

Dimethoxybiphenyls. A mixture containing 4,4′-, 3,4′- and 2,4′-dimethoxybiphenyls was prepared by the method of Abramovitch and Koleoso.[66] 4-Methoxybenzenediazonium tetrafluoroborate, **1**, (0.222 g) was added to a mixture of pyridine (0.237 g), methoxybenzene (22 cm^3) and sulfolane (10 cm^3) and stirred for 1 h at ambient temperature then, under nitrogen, heated at 60 °C for 7 h. The excess of methoxybenzene was removed by vacuum distillation and the residue extracted into ether; sulfolane was removed from the ether extract by repeated water washes. GC-MS analysis of the products revealed only three compounds having M$^+$ 214. The 4,4′-isomer was recognised by comparison of its retention time and mass spectrum with that of commercial material; the 2,4′-isomer was distinguished by the fact that its mass spectrum exhibited an *ortho* fragmentation pattern (loss of 30 mass units, representing CH_2=O, from the molecular ion) producing a peak at m/z 184 shown by neither of the other isomers. For given chromatographic conditions, identifying retention times could therefore be assigned to each isomer. In quantifying these isomeric products, the response factor determined for the 4,4′-isomer was assumed to be applicable to the other two.

Precipitated copper salt. A pale blue precipitate of a Cu^{2+} salt was formed in the product-study experiments. Its IR spectrum in Nujol mull was similar, but not identical, to that of the precipitate obtained by addition of a solution of $Cu(NO_3)_2$ to a solution of either KH_2PO_4 or K_2HPO_4 in 50% v/v aqueous MeCN. It was very similar, however, to that of the precipitate obtained from addition of a solution of $Cu(NO_3)_2$ to a solution of K_2HPO_4 and $NaBF_4$ in the same solvent. Although we have not attempted to establish an accurate stoichiometry, we infer the precipitate to be mixed phosphate–tetrafluoroborate; there is no evidence of associated MeCN. Precipitate from product studies: ν_{max}(Nujol)/cm^{-1} 3371, 1152, 1061, 993; synthetic mixed salt: ν_{max}(Nujol)/cm^{-1} 3354, 1155 (sh), 1065, 996; simple phosphate: ν_{max}(Nujol)/cm^{-1} 3352, 1159, 1071, 1026, 926.

Data Treatment. Non-linear regressions were carried out using *Origin*®, version 6.1 software, OriginLab Corporation, 1991–2000, Northampton MA 01060, USA and linear regressions using *Essential Regression*[67] an add-in for the Microsoft Excel spreadsheet.

Acknowledgements

We are indebted to Mr P. Elliott for the thermal analysis of $[Cu^I(NCMe)_4]$ BF_4, to Mr D. Bettany and Mr Z. ul-Haq for technical assistance and to Dr A. C. Whitwood for help with IT and useful advice. We are grateful to Great Lakes Fine Chemicals and the EPSRC for a Case Studentship (ABT).

References

1 P. Hanson, S. C. Rowell, P. H. Walton and A. W. Timms, *Org. Biomol. Chem.*, 2004, **2**, 1838.
2 (*a*) W. A. Cowdrey and D. S. Davies, *Q. Rev. Chem. Soc.*, 1952, **6**, 358; (*b*) E. Pfeil and O. Vellten, *Justus Liebigs Ann. Chem.*, 1949, **565**, 183.
3 (*a*) S. C. Dickerman, K. Weiss and A. K. Ingberman, *J. Org. Chem.*, 1956, **21**, 380; (*b*) J. K. Kochi, *J. Am. Chem. Soc.*, 1957, **79**, 2942.
4 T. Cohen and A. H. Lewin, *J. Am. Chem. Soc.*, 1966, **88**, 4521.
5 T. Cohen, R. J. Lewarchik and J. Z. Tarino, *J. Am. Chem. Soc.*, 1974, **96**, 7753.
6 J. K. Kochi, in *Free Radicals*, ed. J. K. Kochi, Wiley-Interscience, New York, N. Y., 1973, vol. I, ch. 11.
7 P. Hanson, J. R. Jones, A. B. Taylor, P. H. Walton and A. W. Timms, *J. Chem. Soc., Perkin Trans. 2*, 2002, 1135.
8 (*a*) M. Freiberg and D. Meyerstein, *J. Chem. Soc., Chem. Commun.*, 1977, 127; (*b*) M. Freiberg and D. Meyerstein, *J. Chem. Soc., Faraday Trans. 1*, 1980, **76**, 1825; (*c*) M. Freiberg and D. Meyerstein, *J. Chem. Soc., Faraday Trans. 1*, 1980, **76**, 1838.
9 G. V. Buxton and J. C. Green, *J. Chem. Soc., Faraday Trans. 1*, 1978, **76**, 697.
10 G. Ferraudi, *Inorg. Chem.*, 1978, **17**, 2506.
11 (*a*) H. Cohen and D. Meyerstein, *Inorg. Chem.*, 1986, **25**, 1505; (*b*) N. Navon, G. Golub, H. Cohen and D. Meyerstein, *Organometallics*, 1995, **14**, 5670.

12 N. Shaham, H. Cohen, R. van Eldik and D. Meyerstein, *J. Chem. Soc., Dalton Trans.*, 2000, 3356.
13 (*a*) E. S. Lewis and H. Suhr, *Chem. Ber.*, 1958, **91**, 2350; (*b*) H. Zollinger, in *Diazo Chemistry I: Aromatic and Heteroaromatic Compounds*, VCH, Weinheim, 1994, ch. 5.
14 M. L. Crossley, R. H. Kienle and C. H. Benbrook, *J. Am. Chem. Soc.*, 1940, **62**, 1400.
15 The method of G. J. Kubas, *Inorg. Synth.*, 1990, **28**, 68 for the hexafluorophosphate was adapted for the tetrafluoroborate.
16 C. Diaz, J.-P. Gisselbrecht, M. Gross, J. Suffert and R. Zeissel, *J. Organomet. Chem.*, 1991, **401**, C54.
17 W.-Y. Ng, *J. Chem. Educ.*, 1988, **65**, 727.
18 C. Galli, *J. Chem. Soc., Perkin Trans. 2*, 1981, 1459.
19 P. G. Jones and O. Crespo, *Acta Crystallogr., Sect. C: Cryst. Struct. Commun.*, 1998, **54**, 18.
20 (*a*) P. Hemmerich and C. Sigwart, *Experientia*, 1963, **19**, 488; (*b*) A. Zuberbühler, *Helv. Chim. Acta*, 1970, **53**, 473; (*c*) A. Günter and A. Zuberbühler, *Chimia*, 1970, **24**, 340.
21 U. Bertocci and D. D. Wagman, in *Standard Potentials in Aqueous Solution*, ed. A. J. Bard, R. Parsons and J. Jordan, IUPAC, Marcel Dekker Inc., New York and Basel, 1985, p. 292.
22 Reduction potentials of 0.34 V and 0.41 V have been quoted for the complexes having $n = 1$ and 2, respectively: N. Navon, A. Burg, H. Cohen, R. van Eldik and D. Meyerstein, *Eur. J. Inorg. Chem.*, 2002, 423.
23 P. Hanson, S. C. Rowell, A. B. Taylor, P. H. Walton and A. W. Timms, *J. Chem. Soc., Perkin Trans. 2*, 2002, 1126.
24 (*a*) J. Barbosa and V. Sanz-Nebot, *Anal. Chim. Acta*, 1991, **244**, 183; (*b*) J. Barbosa, R. Bergés, V. Sanz-Nebot and I. Toro, *Anal. Chim. Acta*, 1999, **389**, 43; (*c*) J. Barbosa, I. Marqués, G. Fondrodona, D. Barrón and R. Bergés, *Anal. Chim. Acta*, 1997, **347**, 385; (*d*) J. Barbosa, I. Marqués, D. Barrón and V. Sanz-Nebot, *Trends Anal. Chem.*, 1999, **18**, 543; (*e*) J. Barbosa and V. Sanz-Nebot, *J. Chem. Soc., Faraday Trans.*, 1994, **90**, 3287.
25 A. D'Aprano and R. M. Fuoss, *J. Phys. Chem.*, 1969, **73**, 400.
26 P. W. Atkins, in *Physical Chemistry*, Oxford University Press, Oxford, 4th edn, 1992, p. 861.
27 If individual buffer ratios, as opposed to their mean, are used for corrections to I_{50} in Table 4, the value of $z_i z_j$ obtained, $-(2.27 \pm 0.20)$, is not significantly different.
28 The quasi-third order rate constant $l_{3(50)}$ approximates the true third order constant $k_{3(50)} = (1.81 \pm 0.13) \times 10^3$ dm^6 mol^{-2} s^{-1}, see Results (iv).
29 We have previously described[23] the gas-displacement cell used which is an adaptation of one reported in the literature: M. L. Crossley, R. H. Kienle and C. H. Benbrook, *Ind. Eng. Chem., Anal. Ed.*, 1940, **12**, 216.
30 See ref. 13b, pp. 222–225.
31 A. H. Lewin and T. Cohen, *J. Org. Chem.*, 1967, **32**, 3844.
32 We had found ~10% experimental error was typical during use of the same gas-cell in our investigation of Sandmeyer cyanation, ref. 23.
33 (*a*) M. Cygler, M. Przybylska and R. M. Elofson, *Can. J. Chem.*, 1982, **60**, 2852; (*b*) C. Rømming and T. Tjornhorn, *Acta Chem. Scand.*, 1968, **22**, 2934.
34 (*a*) T. Suehiro, T. Tashiro and R. Nakausa, *Chem. Lett.*, 1980, 1339; (*b*) T. Suehiro, S. Masuda, T. Tashiro, R. Nakausa, M. Taguchi, A. Koike and A. Rieker, *Bull. Chem. Soc. Jpn.*, 1986, **59**, 1877.
35 M. N. Weaver, S. Z. Janicki and P. A. Petillo, *J. Org. Chem.*, 2001, **66**, 1138.
36 M. P. Doyle, C. L. Nesloney, M. S. Shanklin, C. A. Marsh and K. C. Brown, *J. Org. Chem.*, 1989, **54**, 3785.
37 P. Hanson, R. C. Hammond, P. R. Goodacre, J. Purcell and A. W. Timms, *J. Chem. Soc., Perkin Trans. 2*, 1994, 691.
38 J. C. Scaiano and L. C. Stewart, *J. Am. Chem. Soc.*, 1983, **105**, 3069.
39 (*a*) W. A. Waters, *J. Chem. Soc.*, 1942, 266; (*b*) M. C. Ford, W. A. Waters and H. T. Young, *J. Chem. Soc.*, 1950, 833.
40 F. Minisci, F. Coppa, F. Fontana, G. Pianese and L. Zhao, *J. Org. Chem.*, 1992, **57**, 3929.
41 (*a*) C. J. Heighway, J. E. Packer and R. K. Richardson, *Tetrahedron Lett.*, 1974, 4441; (*b*) J. E. Packer, C. J. Heighway, H. M. Miller and B. C. Dobson, *Aust. J. Chem.*, 1980, **33**, 965.
42 R. W. Alder, R. Baker and J. M. Brown, in *Mechanism in Organic Chemistry*, Wiley-Interscience, London, 1971, p. 294.
43 We write formulae of complexes with established coordination conventionally with square brackets [] but use () and {} for postulated complexes where the full coordination is uncertain.
44 (*a*) A. Katagiri, S. Yoshimura and S. Yoshizawa, *Inorg. Chem.*, 1981, **20**, 4143; (*b*) A. Katagiri, S. Yoshimura and S. Yoshizawa, *Inorg. Chem.*, 1986, **25**, 2278.
45 Since radical and nucleophilic additions to benzenediazonium ion normally take place at N_β or conjugated ring positions, we discount *ipso*-attack on **1** either by An$^\bullet$ or by a nucleophilic organocopper intermediate as routes to **4**. The nearest precedent for *ipso*-attack would be Ullmann reaction in which aryl halides are coupled to give biaryls on reaction with copper metal at high temperature. Organocopper intermediates are involved: T. Cohen and I. Cristea, *J. Am. Chem. Soc.*, 1976, **98**, 748, but we consider it implausible that a diazonium group could mimic a halogen in an Ullmann-like reaction and doubt the relevance of Ullmann-type reaction to the formation of the symmetrical 4,4′-dimethoxybiphenyl, **4**, here.
46 F. A. Bolth, W. M. Whaley and E. B. Starkey, *J. Am. Chem. Soc.*, 1943, **65**, 1456.
47 (*a*) Although aryl radicals are known to be highly reactive towards O_2 [Z. B. Alfassi, S. Marguet and P. Neta, *J. Phys. Chem.*, 1994, **98**, 8019; (*b*) X. Fang, R. Martens and C. von Sonntag, *J. Chem. Soc., Perkin Trans. 2*, 1995, 1033.], we also exclude any significant role for atmospheric oxygen in the production of **6** as product distributions were scarcely affected by its exclusion.
48 D. F. Shriver, P. W. Atkins and C. H. Langford, in *Inorganic Chemistry*, Oxford University Press, Oxford, 1991, p. 211.
49 *Simula*: a kinetic simulation programme adapted from prior software (*Chekin*) made available by Professor D. J. Waddington, and subsequently further adapted by Dr A. C. Whitwood, to run on IBM compatible personal computers, University of York.
50 See ref. 26, p. 795.
51 O. Brede, R. Mehnert, W. Naumann and H. G. O. Becker, *Ber. Bunsen-Ges. Phys. Chem.*, 1980, **84**, 672.
52 I. Fleming, in *Frontier Orbitals and Organic Chemical Reactions*, Wiley-Interscience, Chichester, 1976, p. 186.
53 R. Glaser and C. J. Horan, *J. Org. Chem.*, 1995, **60**, 7518.
54 J. Bargon and K.-G. Seifert, *Tetrahedron Lett.*, 1974, 2265.
55 (*a*) C. J. Rhodes, *J. Chem. Soc., Chem. Commun.*, 1990, 799; (*b*) C. J. Rhodes, H. Agirbas, M. Lindgren and O. N. Antzukin, *J. Chem. Soc., Perkin Trans. 2*, 1993, 2135.
56 (*a*) R. F. Gunnion, M. K. Gilles, M. L. Polak and W. C. Lineberger, *Int. J. Mass Spectrom. Ion Processes*, 1992, **117**, 601; (*b*) G. B. Ellison, P. C. Engleking and W. C. Lineberger, *J. Am. Chem. Soc.*, 1978, **100**, 2556 both given at http://webbook.nist.gov./cgi/cbook.
57 (*a*) J. C. Scaiano, W. J. Leigh and G. Ferraudi, *Can. J. Chem.*, 1984, **62**, 2355; (*b*) A. Mayouf, H. Lemmetyinen, I. Sychttchikova and J. Koskikallio, *Int. J. Chem. Kinet.*, 1992, **24**, 579.
58 R. M. Smith, A. E. Martell and R. J. Motekaitis, *NIST Standard Database 46: NIST Critically Selected Stability Constants of Metal Complexes, Version 8 for Windows, May*, 2004, National Institute of Standards and Technology, Standard Reference Data Program, Gaithersburg, MD, 20899.
59 D. Griller, D. Schmid and K. U. Ingold, *Can. J. Chem.*, 1979, **57**, 832.
60 P. Hanson, J. R. Jones, B. C. Gilbert and A. W. Timms, *J. Chem. Soc., Perkin Trans. 2*, 1991, 1009.
61 See ref. 13b, p. 200.
62 An EPR spectrum originallyassigned to $PhN_2^\bullet$ (W. T. Dixon and R. O. C. Norman, *J. Chem. Soc.*, 1964, 4857) was subsequently suggested to be due to PhN=NPh$^{+\bullet}$ (see ref. 54) but this has been questioned (see ref. 55 and also; E.-L. Dreher, P. Niederer, A. Rieker, W. Schwarz and H. Zollinger, *Helv. Chim. Acta*, 1981, **64**, 488).
63 (*a*) E. R. Atkinson, H. J. Lawler, J. C. Heath, E. H. Kimball and E. R. Read, *J. Am. Chem. Soc.*, 1941, **63**, 730; (*b*) E. R. Atkinson, C. R. Morgan, H. H. Warren and T. J. Manning, *J. Am. Chem. Soc.*, 1945, **67**, 1513; (*c*) E. R. Atkinson and D. M. Murphy, *Org. Synth. Coll. Vol. IV*, 1963, 872; (*d*) E. R. Atkinson and H. J. Lawler, *Org. Synth. Coll. Vol. I, 2nd edn*, 1964, 222.
64 R. M. Silverstein and F. X. Webster, in *Spectrometric Identification of Organic Compounds*, Wiley, New York, N. Y., 6th edn, 1998, p. 7.
65 (*a*) J. P. Otruba and R. G. Weiss, *J. Org. Chem.*, 1983, **48**, 3448; (*b*) M. C. Carreño, G. Fernández Mudarra, E. Merino and M. Ribagorda, *J. Org. Chem.*, 2004, **69**, 3413.
66 R. A. Abramovitch and O. A. Koleoso, *J. Chem. Soc. B*, 1969, 779.
67 D. D. Steppan, J. O. Werner and R. P. Yeater, *Essential Regression*, 1998 and 2006, add-in for Microsoft Excel, freely available at http://www.geocities.com/jowerner98/index.html.

